D2-expressing neurons of the anterior paraventricular nucleus of the thalamus as key players for modulating relative aversive and safety learning

Magdalena Miranda[1,#], Elsa Karam[1,#], Pola Tuduri[1], Maïwenn Passard[1], Majda Drahmani[1], Loic Vaillant[1], Christina-Anna Vallianatou[1], Marina Lavigne[2], Eric J. Kremer[2], Jeanne Ster[1], Emmanuel Perisse[1,#,*] and Stéphanie Trouche[1,3,#,*]

[1] Institute of Functional Genomics, University of Montpellier, CNRS, INSERM, Montpellier, France.

[2] Institute of Molecular Genetics of Montpellier, University of Montpellier, CNRS, Montpellier, France.

[3] Lead contact

[#] These authors contributed equally to this work

* Correspondence: stephanie.trouche@igf.cnrs.fr and emmanuel.perisse@igf.cnrs.fr

Keywords: avoidance, defensive strategies, safety, aversive value, D2 receptor-expressing neurons, PVT.

Abstract

Associative learning provides a means to assign appropriate value signals to experiences that animals can later use to make appropriate value-based choices. By generalizing from prior aversive experiences and comparing with a current experience, animals can learn the relative aversive ("better or worse than") value or relative positive safety value between experiences. Yet, how such relative value signals are acquired during learning remain poorly known. The paraventricular nucleus of the thalamus (PVT) is critical for the control of salience and valence signals. It is therefore well-placed to be involved in learning relative aversive value and learned safety. Using a newly-developed conditioned place preference task, we uncover specific behavioral signatures associated with learning relative aversive value and learned safety, and related value-based choices. We then show that neurons expressing dopamine D2 receptor (D2+) in the anterior PVT (aPVT) are preferentially recruited by both relative aversive value learning and learned safety. Using a pharmacogenetic strategy, we demonstrate that aPVT D2+, but not D2-, neurons are involved in learning relative- but not absolute- aversive value. Finally, we show that aPVT D2+, but not D2-, neurons are also critical for the encoding of learned safety. Overall, our findings reveal a novel role of aPVT D2+ neurons in computing relative aversive/safety value signals between experiences during learning to promote appropriate value-based choices.

Introduction

Learning that some cues can predict threat while others can predict safety is critical for appropriate decision-making and survival. [1–3] By generalizing predictions [4,5] and comparing the value of contextual/sensory signals of a prior aversive experience with an ongoing threat, animals can learn the relative aversive value between two experiences (i.e. whether one is better or worse than the other). [6–11] However, by generalizing prediction and comparing a prior aversive experience with the absence of a threat, animals can learn relative safety. [12–14] Moreover, previous studies showed that learning the relative aversive value between two aversive experiences, such that one is perceived as better than the other, involves the reward system.[6,7,15] Similarly, a safe experience, relative to a prior aversive one, can acquire a relative positive value called learned safety, a process that also requires the reward system. [16,17] When later confronted with a choice between two options, pre-computed values acquired during learning (here relative aversive value or learned safety) facilitate decision-making processes,

thus promoting more efficient and accurate value-based choices. [18] Critically, overgeneralization and dysregulation of a normal threat and safety learning, leading to alteration of relative value computation, is maladaptive and serves as a major feature of fear-related disorders including post-traumatic stress disorder (PTSD). [4] While fear generalization [4,19] and the interaction between appetitive and aversive systems [7,20–22] are likely crucial players in the encoding of value signals, how the comparison of generalized predicted and current values contribute to the encoding of relative aversive value and learned safety remains poorly understood.

The paraventricular nucleus of the thalamus (PVT) is a hub connecting the thalamus with cortical and limbic structures [23–27], which is critically involved in arousal, stimulus salience processing and value assignment to associative stimuli. [28,29] [30–33] The PVT is therefore a strong candidate structure for disentangling motivational conflicts and comparing experiences to compute appropriate relative value signals during learning. [24,28,33–37] Due to its involvement in granting and updating the value of aversive experiences [28,36,38–42], here we hypothesize that the PVT is crucial for the assignment of a relative aversive/safety value. Of note, the D2 dopamine receptor-expressing neurons (D2+) of the PVT are sensitive to valence [33] and are implicated in signaling aversive states. [33,39] By contrast, D2-non-expressing neurons (D2-) are modulated by arousal, relaying a salience signal to the cortex. [33] According to this functional dissociation, D2+ neurons could be critical to signal a “better than expected” relative aversive value. The PVT is also instrumental for the correct assignment of a learned safety value to an experience. [42] However, it remains unclear whether D2+ neurons of the PVT differentially contribute to encoding relative aversive value and/or learned safety.

Here, we addressed this question by designing a novel conditioned place preference task that allows mice to encode either relative aversive value or learned safety. In this task, mice learn to associate one context with foot shock delivery, followed by a second context that is either associated with shocks of lower intensity (learning a relative “better” aversive value), or with the absence of shocks (for learned safety). After learning, mice are confronted to a choice between the two contexts. We showed that mice adapt their defensive responses to each task, exhibiting distinct behavioral signatures during learning and choice tests. Our data revealed that during learning of the second context, when comparing it to the previous aversive experience, both tasks preferentially recruit D2+ neurons in the aPVT compared

to pPVT. We then found that pharmacogenetic inactivation of aPVT D2+, but not D2-, neurons during the exposure to the second context disrupt relative aversive comparison by increasing its aversiveness. This led to a suppressed preference towards the less punished-associated context during the choice test. Consistently, when mice learn to associate two distinct contexts paired with the same shock intensity, inactivation of aPVT D2+ neurons during the exposure to the såecond context also increases its aversiveness, tilting mouse preference towards the first context during choice test. Finally, we found that inactivating aPVT D2+ neurons increases safety of the ongoing experience inducing enhanced preference towards the safe context during choice test.

Taken together, our data demonstrate that aPVT D2+ neurons modulate the comparison of values during learning that enables accurate assignment of relative aversive value and learned safety, thereby promoting appropriate value-based choices. These results also provide compelling evidence that aPVT neuronal ensembles expressing D2 receptors, embedded within limbic-cortical circuits, are key in the evaluation process for assigning correct value signals to sensory experience during associative learning.

Results

Mice use different behavioral strategies for learned relative safety and relative aversive value-based learning and choice

To study the neural circuits and mechanisms underlying learned safety and relative aversive value coding, we designed a novel 1-day conditioned place preference (CPP) task **(Figures 1A** and **S1A**). In this task, mice are subjected to a pretest session ("Pretest"), allowing them to explore two never-encountered contexts (A and B connected via a bridge) followed by two conditioning sessions ("S1" and "S2") in each context, and a test session ("Choice test") between contexts A and B. Three groups were tested. In the control group, no shock was delivered in any context during S1 and S2. To study learned relative safety value (named the “safe” group), we employed a discriminative/differential fear conditioning paradigm [12–14] during which mice received four electric shocks of 0.6 mA in context A during S1 ("A+0.6"), but no shock (no threat) in context B during S2 ("B+0"). To study learned relative aversive value (named the “aversive” group), mice were subjected to four electric shocks of 0.6 mA in context A during S1 ("A+0.6") as for the safe group, but received four electric shocks of 0.3 mA in context B during

109 S2 ("B+0.3"). As expected, no freezing was observed during Pretest in any group (**Figure S1B**). Both
110 safe and aversive groups exhibited increased freezing levels in S1 and S2 conditioning sessions
111 compared to the control group (**Figure S1C**). However, only mice in the aversive group showed
112 increased freezing from S1 to S2 **(Figure 1B**), along with heightened anxiety as measured with a
113 decreased time spent in the center during S2 (**Figure S1D**). By analyzing the dynamic of freezing during
114 S1 and S2 (**Figures S1E**), we found that freezing before the putative first shock of S2, but not S1,
115 significantly increased for both safe and aversive groups compared to control group (**Figure 1C**). The
116 increased freezing observed at the beginning of S2 suggests a generalized expectation based on their
117 previous aversive experience in context A+0.6 mA. Importantly, while both aversive and safe groups
118 increased freezing after the 4th (and last) shock in S1 (**Figures 1D, S1E** and **S1F**), only mice in the
119 aversive group maintained a high freezing level at the end of S2 (i.e., after receiving four shocks in
120 context B), indicating that the aversive group learned that context B is aversive (**Figures 1D** and **S1E**).
121 In contrast, mice in the safe group significantly decreased their freezing after the fourth (and last)
122 putative shock (**Figure 1D**) suggesting that mice start to discriminate both contexts, perceiving context
123 B+0 mA as relatively safer than context A + 0.6 mA. Strikingly, we also observed tail rattling behavior
124 only in the aversive group immediately after each shock event in S2 (**Figure 1E; video 1**), but not S1
125 (**Figure S1G**). Thus, the increased number of shock events shifted mouse's defensive responses. The
126 absence of such active defensive behavior in response to a threat [43] in the safe group strengthen the
127 idea that context B + 0 mA became relatively safer than context A+0.6 mA. Overall, our results indicate
128 that relative to a prior intense aversive experience, mice assign a relative aversive/safe value to ensuing
129 less punished/not punished experience.
130 One hour after the learning phase, all mice were tested during a choice-test session. Importantly, mice
131 were first placed in their most preferred context (defined during Pretest), i.e., context A_0 for the control
132 group and the most punished Context $A_{0.6}$ for both safe and aversive groups (**Figure 2A)**. Their latency
133 to cross from context A to context B (i.e., First latency) was similar between all 3 groups during choice
134 test (**Figure S2A**). Similarly, the number of tail rattling was similar before their first cross to context B
135 (**Figure S2B; video 2**). However, only mice from the aversive group spent more time in the bridge
136 before the first cross (**Figures 2B** and **2C**). In addition, the majority of mice in the aversive group (10
137 out of 12) displayed a "turn-back" behavior in the bridge zone (**Figure 2D; video 3**). Such behavioral

138 signature is reminiscent of the "vicarious trial and error" behavior with animals moving back and forth in
139 direction of different choices at decision zones. [44,45]
140 After crossing the bridge for the first time (i.e., First cross), mice were allowed to explore the two
141 contexts for 15 min (as in [46,47]) (**Figure S2C**). We calculated a ΔCPP score comparing the time spent
142 in each context during pretest (15 min, **Figure S2D**) vs choice test (15 min after first cross, **Figure 2E**).
143 As expected, control mice showed no preference for either of the two contexts during choice test (ΔCPP
144 score close to zero, **Figure 2E**). Mice from the safe and aversive groups similarly reverted their initial
145 preference and spent more time in the less aversive context (positive ΔCPP score significantly different
146 from zero and not significant between safe and aversive groups, **Figure 2E**), along with a reduced
147 exploratory behavior (**Figures S2C** and **S2E**). Their preference was similar for both safe and aversive
148 groups during the first 5 min of the test, but was sustained in the aversive group throughout the choice
149 test (**Figure S2F**). For the aversive group, this preference was accompanied with increased freezing in
150 the bridge zone and context $B_{0.3}$ (**Figure 2F**), along with higher stress marked by more feces (**Figure**
151 **S2G**). In line with these results, the aversive group stayed longer in the bridge after the first cross
152 (**Figure 2G**). These data suggest that the aversive group therefore utilized prior learning information to
153 avoid the most punished context $A_{0.6}$ and potentially approach context $B_{0.3}$ [15] while being anxious and
154 showing hesitation to make a choice between the two aversive contexts. By contrast, the safe group
155 preferred the safe B_0 context and showed less anxiety-like behavior. Overall, mice use learned
156 experience to adopt specific behavioral signatures and enable appropriate value-based choices.
157
158 **Both learned relative safety and relative aversive learning preferentially recruit D2+ neurons in**
159 **the aPVT**
160 We hypothesized that mice compare the relative value of the two experiences during conditioning S2
161 relative to S1 and assign either a relative "better than" aversive value to context B (paired 0.3 mA
162 shocks) for the aversive group [6,7,34] or a relative safety value to context B (no threat) for the safe group.
163 [12,14,17] However, it remains unclear how mice encode a relative value (aversive or safe) between
164 experiences, and how this influences subsequent value-based choices. The PVT is central for
165 modulating anxiety-related conflicting appetitive-aversive information [37,48] and could be pivotal for the
166 encoding of relative (aversive or safe) value. Notably, the functional PVT antero-posterior axis
167 expressing dopaminergic D2 receptor (D2+ neurons) involved in salience and valence coding [33,49,50]

168 could extricate the different intensities of prior (during S1) and actual information learned during the
169 conditioning session S2. We first tested this hypothesis by asking whether PVT neurons, in particular
170 D2+ neurons, are differentially recruited during learning using D2 Cre:Ai14 mice (see Methods). First,
171 our *ex vivo* whole-cell recording experiments confirmed that td-Tomato (i.e., Ai14) cells respond to
172 quinpirole (D2R-like agonist, 1□M; action potential (AP) frequency baseline = 1.00 +/- 0.20 Hz, AP
173 frequency quinpirole = 0.37 +/- 0.21 Hz, n= 5 cells, paired t-test p= 0.0047 **) validating the use of this
174 mouse line. We then performed a cFos immunostaining in the aPVT and pPVT in D2-tagged animals
175 of 3 groups: home-cage (HC), safe and aversive (**Figures 3A** and **3B**). To reflect cFos activity at the
176 time of the comparison between the two conditioning sessions, mice were perfused 90 min after the
177 conditioning session S2. Importantly, we verified that both safe and aversive groups showed distinct
178 freezing patterns at the end of S2 (**Figures S3A** and **S3B**), as we previously described (**Figures 1C**
179 and **1D**). We found that both safe and aversive groups show similar, and significantly higher, levels of
180 activated (cFos positive) neurons compared to the home-cage group (**Figure 3C**). In the safe and
181 aversive groups, such recruitment was more prominent in the aPVT than the pPVT (**Figures 3C** and
182 **S3C**) and incorporated a higher proportion of D2+ than D2- neurons in the aPVT, but not pPVT (**Figures**
183 **3D-3E**). Noteworthy, D2+ cell densities were similar between all groups, but were higher in pPVT than
184 aPVT **(Figure S3D)**, as previously published. [33] These results indicate that both learned safety and
185 relative aversive learning recruit preferentially aPVT D2+ neurons. Mice were subjected to a choice test
186 immediately before being perfused (**Figures 3A**)**.** In line with our previous findings (**Figure 2E)**, both
187 safe and aversive groups significantly preferred the non-punished (context B_0) or less punished
188 compartment (context $B_{0.3}$) during choice test, respectively (positive ΔCPP score in **Figure S3E**). As
189 shown in **Figure 2**, the relative choice between the two previously (and differently) punished contexts,
190 $A_{0.6}$ and $B_{0.3}$, led mice to spend a prolonged period in the bridge, likely assessing the two aversive
191 options to make an appropriate choice (**Figure S3F**). Given the role of the PVT and the increased
192 activation of D2+ neurons during the conditioning session S2, we hypothesized that mouse behavior
193 during the choice test is closely linked to the activity of aPVT D2+ neurons during S2. Accordingly, the
194 percentage of activated D2+ neurons of the aPVT (but not pPVT) of the aversive group during S2 is
195 negatively correlated with the time spent on the bridge (i.e., the decision zone) during the choice test
196 (**Figure 3F**). In other words, the less aPVT D2+ neuron activation during S2, the more time mice will
197 spend in the bridge at the start of the choice test. Strikingly, such correlation was not observed for aPVT

198 D2-negative activated neurons (**Figure 3F**), nor for the safe group (**Figure 3G**). These results strongly
199 suggest a crucial role of aPVT D2+ neurons for learning relative aversive value during conditioning to
200 subsequently promote an appropriate relative aversive value-based choice.
201
202 **aPVT D2+, but not D2-, neurons are crucial for learning relative aversive value**
203 To directly test the role of aPVT D2+ neurons for learning relative aversive value during conditioning in
204 S2, we virally injected D2 Cre mice with viral vectors expressing a Cre-dependent DREADD (AAV-DIO-
205 hM4Di-mCherry) or control viral vector (AAV-DIO-mCherry) in the aPVT (**Figure 4A**). Four weeks later,
206 mice underwent the aversive CPP task and were injected with Clozapine N-Oxide (CNO)
207 intraperitoneally 30 min before S2. This pharmacogenetic strategy aimed to inactivate aPVT D2+
208 neurons when mice relatively compare the S1 and S2 experiences (**Figure 4B**). To ascertain the effect
209 of hM4Di activity, we performed *ex vivo* whole-cell recordings in control- and hM4Di-D2+ neurons of
210 the aPVT, identified by their mCherry fluorescence (**Figure S4A)**. The application of 10□M CNO to
211 aPVT brain sections expressing inhibitory DREADD (hM4Di) hyperpolarizes D2+ neurons by drastically
212 decreasing spike frequency (**Figure S4A)**. By contrast, CNO had no impact on aPVT D2+ neurons
213 transduced with the control AAV-DIO-mCherry virus (**Figure S4A)**. In line with previous reports, we also
214 confirmed projection targets of aPVT D2+ neurons such as nucleus accumbens (NAc) and amygdala
215 (**Figure S4B**). [33] First, and as expected, both control and hM4Di groups showed a similar preference of
216 context during pretest before CNO injection (**Figure S4C).** While silencing aPVT D2+ neurons during
217 S2 did not change the amount of freezing during conditioning (**Figures S4D** and **S4E**), it led to a
218 significant increase of tail rattling behavior in S2 for the hM4Di group immediately after receiving electric
219 shocks (**Figure 4C**). Moreover, while we observed a decreased average distance travelled after shock
220 delivery between S1 and S2 in the control group (**Figure 4D**), inhibiting aPVT D2+ neurons prevented
221 such decrease during S2 (**Figure 4D**). These findings suggest that silencing aPVT D2+ neurons
222 heightened shock perception during S2, thereby possibly increasing the aversiveness of context B+0.3.
223 As a consequence, before their first cross from context $A_{0.6}$ to context $B_{0.3}$ during choice test, mice
224 displayed a higher number of turnbacks (**Figure 4E**) and tail rattling (**Figure 4F**) in the bridge without
225 changing their first latency to cross (**Figure S4F**) nor the time they spent in the bridge zone (**Figure**
226 **S4G**). These results indicate that hM4Di mice perceived context $B_{0.3}$ as threatening as context $A_{0.6}$. In
227 line with this conclusion, the preference of control mice for the previously less punished context $B_{0.3}$

228 was fully suppressed in hM4Di mice (ΔCPP score close to 0; **Figure 4G**). This was true when aPVT
229 D2+ neurons were inactivated during S2, but not during choice test, highlighting the selective role of
230 aPVT D2+ neurons for relative aversive value-based learning (**Figure S4H-J**). hM4Di mice spent more
231 time in the bridge zone after their first cross from context $A_{0.6}$ to context $B_{0.3}$ (**Figure 4H**), indicating
232 more hesitation to choose between the two contexts. Moreover, mice froze less in context $B_{0.3}$ (**Figure**
233 **4I;** also see **Figure 2E**). Overall, our results converge towards the idea that silencing aPVT D2+
234 neurons enhanced the aversiveness of the "context B+0.3 mA" learning experience to reach a similar
235 aversiveness as in context A+0.6 mA. This would therefore prevent mice from accurately learning the
236 relative difference between two aversive experiences and from assigning a relative "better than"
237 aversive value to context B+0.3 mA. In line with this hypothesis, conditioning mice to contexts A and B
238 both paired with 0.6 mA (**Figure S4K**) led to similar results, with notably a similar tail rattling during S1
239 and S2 and a similar distance travelled after shock between S1 and S2 (**Figures S4L** and **S4M**). In
240 addition, we observed similar consequences during the choice test with notably a ΔCPP score not
241 different from 0 and similar freezing in $A_{0.6}$, bridge and $B_{0.6}$ (**Figures S4N** and **S4O**). We thus propose
242 that aPVT D2+ neurons are critical to compare the relative aversiveness between the two experiences
243 during learning, thereby contributing to the encoding of relative aversive value and triggering
244 appropriate threat-related behavior.
245 To address whether D2+ neurons are specifically required for relative aversive value coding, but not for
246 coding absolute aversive value, we conducted two sets of experiments in which mice could not
247 generalize threat from a prior aversive experience. In the first experiment, mice were subjected to a
248 contextual fear conditioning task (four shocks of 0.3 mA in context B) (**Figures 4J** and **4K**). We found
249 that silencing aPVT D2+ neurons during contextual fear conditioning of context B+0.3 mA, did not alter
250 the aversiveness of the experience as no changes in freezing nor tail rattling during conditioning and
251 test were observed (**Figures 4L-O**). In a second experiment, mice were subjected to an absolute
252 aversive protocol (no shock in context A followed by four shocks of 0.3 mA in context B; **Figure S4P-**
253 **Q**). Again, silencing aPVT D2+ neurons during conditioning of context B+0.3 mA, did not change mouse
254 behavior (**Figures S4R-T**). These data are consistent with a specific role for aPVT D2+ neurons to
255 encode relative aversive value during learning.
256 These results however do not rule out a putative role of aPVT D2- (minus) neurons for the encoding of
257 relative aversive value, considering their role in arousal and responses to stimuli saliency [33], and their

258 increased cFos expression during S2 (although significantly lower than aPVT D2+ neurons; **Figure 3D**).
259 To tackle this question, we employed a viral strategy to specifically target and inactivate aPVT D2-
260 neurons (AAV-FLEx-OFF-hM4Di-mCitrine/mCherry with corresponding control viruses based on [51];
261 **Figure 5A, Figure S5A** and methods). We first tested the efficiency of the vector by performing *ex vivo*
262 whole-cell recordings in control- and hM4Di-D2- neurons of the aPVT, identified by their fluorescence
263 (**Figure S5A)**. Our data confirmed that bath application of 10□M CNO to aPVT brain sections
264 expressing inhibitory DREADD (hM4Di) hyperpolarizes D2- neurons by drastically decreasing spike
265 frequency. By contrast, bath application of CNO was ineffective on aPVT D2- neurons transduced with
266 the control virus (**Figures S5B**). We also confirmed the specificity of the FLEx-OFF viral vector to aPVT
267 D2- neurons, with only 3% overlap with D2+ neurons (**Figures S5C** and **S5D**). We next injected CNO
268 30 min before S2 in order to inactivate aPVT D2- neurons during S2 of the aversive task (**Figure 5B**).
269 While hM4Di mice froze slightly less than control before first shock in S2 (**Figures S5E)**, other
270 behavioral parameters previously described remained unchanged during conditioning (including tail
271 rattling, **Figures 5C-D** and **Figures S5F**) nor during choice test (**Figures 5E-I** and **Figures S5G-H)**.
272 Therefore, our results strongly suggest that inactivated aPVT D2+, but not D2- neurons, enhance the
273 relative aversiveness of a threat.
274 Together, we demonstrated that only aPVT D2+ neurons are essential for the encoding of relative
275 aversive value during learning to enable appropriate relative value-based choice.
276
277 **aPVT D2+ neurons dampen relative aversiveness of a threat**
278 To further test our hypothesis that inactivating aPVT D2+ neurons enhances the relative aversive value
279 of the threat-associated context, we conditioned control and hM4Di mice to associate contexts A and B
280 with identical low-intensity shocks (0.3 mA) and administered CNO 30 min before S2 (**Figure 6A**).
281 Confirming our previous findings, silencing aPVT D2+ neurons significantly increased the number of
282 tail rattling post-shock during S2 (**Figure 6B**) without altering the distance travelled after shock (**Figure**
283 **S6A**). Furthermore, and as previously shown in **Figure S4D**, such pharmacogenetic intervention did
284 not change freezing behavior before the first (**Figure S6B**) or after the fourth shock of each conditioning
285 session S1 and S2 (**Figure 6C**). As a consequence, we found that hM4Di mice first placed in $A_{0.3}$ during
286 the choice test displayed more turnbacks in the bridge zone before their first cross to context $B_{0.3}$
287 (**Figure 6D**), with a similar number of tail rattling (**Figure S6C).** Other behavioral parameters were

288 preserved (first latency, **Figure 6E**, time spent in the bridge zone before, **Figure 6F**, and after the first
289 cross, **Figure S6D** and freezing during choice test, **Figure 6G**). However, as shown in **Figure 4G** during
290 choice test**,** hM4Di mice did not prefer either of the two contexts (ΔCPP score not different from 0;
291 **Figures 6H** and **S6E**) compared to control mice. This behavior is likely due to the heightened
292 aversiveness of context $B_{0.3}$ following the inactivation of aPVT D2+ neurons.
293 These results combined with those shown in **Figures 4**, **5**, **S4** and **S5** provide strong evidence for a
294 critical role of aPVT D2+ neurons for modulating the relative comparison of aversive experiences during
295 learning and the encoding of relative aversive value, essential information that mice later use to make
296 appropriate value-based choices.
297
298 **aPVT D2+, but not D2-, neurons are involved in learned relative safety**
299 PVT neurons modulate the salience of both aversive and appetitive behavior [28], a crucial information
300 for both fear and reward learning. [52,53] As we found an increased cFos expression in aPVT D2+ neurons
301 in S2 in the safe group (**Figures 3C-3E**), we next asked whether aPVT D2+ neurons also play a role in
302 learned relative safety, as they do for learning relative aversive value. To test our hypothesis, we
303 subjected control and hM4Di mice to the discriminative fear conditioning (**Figure 1A**) and injected CNO
304 30 min before conditioning S2 in context B+0 mA (**Figure 7A**). In line with our hypothesis, silencing
305 aPVT D2+ neurons did not change threat-related defensive behaviors during conditioning (**Figures 7B-**
306 **C** and **S7A-B**). During choice test, we also found that threat-predicting behavior such as the number of
307 turnbacks and tail-rattling behavior in the bridge zone before going to the non-shocked B_0 context (i.e.
308 before first cross) were also unchanged (**Figures 7D-E**). However, while there were no changes of their
309 first latency to cross from $A_{0.6}$ to B_0 (**Figure 7F**) nor their time spent in the bridge after the first cross
310 (**Figure S7C**), hM4Di mice exhibited a longer latency to go back to the punished context $A_{0.6}$ (second
311 latency, **Figure 7G**). Importantly, hM4Di mice exhibited a higher percentage of freezing/immobility in
312 the safe context B_0 (**Figure 7H**) as they showed a higher preference for the safe context B_0 compared
313 to control mice (**Figures S7D** and **7I**). These data indicate that inactivation of aPVT D2+ neurons during
314 S2 increased safety in context B+0 mA, thus strongly increasing the preference towards the safe context
315 B_0 during the choice test.
316 To verify that inactivating aPVT D2+ neurons during the exposure to context B+0 mA did not assign a
317 positive value to this context during conditioning, control and hM4Di mice were subjected to two novel

318 and distinct contexts (C and D contexts, **Figure S7E**) without shock, and CNO was i.p. injected 30 min
319 before S4 in context D+0. As expected, we did not find any change in any mouse behavior during
320 conditioning or choice test (**Figures S7F-O**).
321 Our results in **Figure 3D** showed an increased cFos expression in aPVT D2- neurons during the
322 encoding of relative safety value, although significantly lower than aPVT D2+ neurons. We therefore
323 asked whether the increased safety we observed reflects the selective inhibition of aPVT D2+ neurons,
324 rather than an overall role of aPVT. To test this hypothesis, aPVT D2- neurons were inactivated during
325 S2 using the same viral strategy as before (**Figures 5** and **7J**). While we found a decreased freezing
326 in S2 for the hM4Di group compared to control mice (**Figure S7P**, as in **Figure S5E**), our results
327 demonstrated that this manipulation had no effect on the capacity of mice to learn a safety value in S2
328 during conditioning nor choosing to stay in the safe context B_0 during choice test (**Figures 7K-R** and
329 **S7 Q-S**).
330 Together, these findings strongly indicate that aPVT D2+, but nor D2-, neurons modulate learned
331 relative safety during conditioning markedly influencing ensuing value-based choice behavior.
332
333 **Discussion**
334 Our study reveals a critical role of aPVT D2+ neurons for learning relative aversive value and learned
335 safety to promote appropriate value-based choices. Using a novel conditioned place preference task,
336 we found that distinct behavioral signatures are associated with learning relative aversive value and
337 learned safety, and related value-based choices. We then demonstrated that learning relative aversive
338 value and learned safety preferentially recruit D2+ neurons in the aPVT compared to that of pPVT.
339 Moreover, inactivating aPVT D2+, but not D2-, neurons at the moment of the comparison between
340 previous aversive and actual aversive/neutral experiences heightened the aversiveness/safeness of
341 the experience. Such enhancement modified learning and then, the selection of subsequent behavior
342 when mice had to choose between the two available options. Importantly, aPVT D2+ neurons modulate
343 relative, but not absolute, aversive value coding, since that in the absence of a prior aversive
344 experience, their pharmacogenetic inactivation did not alter the aversiveness of the ongoing
345 experience. This work provides key findings that improve our understanding of how context-dependent
346 relative (aversive and safe) values are encoded in the brain.
347

aPVT D2+, but not D2-, neurons are key modulators of relative aversive value learning

Extensive work focused on brain mechanisms for relative appetitive learning related to reward and gain. [11,54,54,55,55–65] Surprisingly, the neural circuits underling relative aversive learning and choice remain poorly understood. Here, we designed a novel 1-day conditioned place preference task in which mice learn the association of two distinct contexts with different shock intensities, the first context paired with 0.6 mA and a second context with less intense 0.3 mA shocks. Later, mice are confronted to a choice between the two contexts. Our data showed that this relative aversive task is associated with increased freezing, emergence of tail rattling and decreased time in the center of the context during the second conditioning session. These key behavioural features were restricted to relative aversive value learning, since they were absent in the absence of prior aversive experience. Strikingly, tail rattling is a behavior typically associated with aggression in male mice before fighting. [66] In our set of experiments, tail rattling may therefore be associated with a negative emotional state and a reaction against a possible threat, occurring during learning (i.e. immediately after a negative shock event) but also during memory retrieval (choice test) when mice can make predictions of a possible threat. Previous work has suggested a role of PVT for modulating the value and salience of stimuli. [28,33] Moreover, previous studies highlighted a crucial role of the PVT during motivational conflict scenarios where both approach and defensive behaviors compete. [28,37,48,67] We found that pharmacogenetic inactivation of aPVT D2+, but not D2-, neurons enhances the aversiveness of the ongoing aversive experience demonstrated by both increased tail-rattling and running immediately after each shock. Since tail rattling behavior may increase visual and auditory saliency of the mouse to predators [43], our data suggest that aPVT D2+ neuronal inactivation caused a shift in the defensive behavioral strategy, favoring enhancement of active threat responses.

Our results also revealed that during the relative choice between the two previously punished contexts, mice increased time spent and numerous turnbacks when located in the bridge zone. Such behavior is reminiscent of the “Vicarious Trial and Error” (VTE) phenomenon [44,68] observed at decision point when animals pause and move their head back and forth to “scan” and evaluate the possible outcomes before making a choice between two or more options with uncertain outcomes. [45] Importantly, VTE behavior is preferentially exhibited in hippocampal-dependent tasks and during complex decision making processes. [69–71] Given the critical role of contextual information in our new relative task and the observed PVT-hippocampus anatomo-functional connectivity [23], our newly designed relative aversive

task could serve to expand our knowledge of the neuronal circuits underlying VTE behavior and value-based decision-making processes.

aPVT D2+ neurons modulate predictive signals for learning aversive value and learned safety. The PVT is widely recognized as signaling aversive states and modulating fear-related behaviors [23,28,33,36,38,41,72–74], as well as appetitive associative learning [28,75], and reward-seeking behavior. [76–78] Moreover, PVT neurons are activated by cues or contexts previously associated with positive or negative emotional outcomes. [23,36–38,73,76,79–84] In the safe condition, in which the first context is paired with 0.6 mA shocks followed by a second context in which no shocks are delivered (a differential/discriminative conditioning), animals likely acquire a learned safety. [4,12–14] Our cFos staining revealed that the aPVT is more recruited than pPVT by both a second context paired with a weaker shock (relative aversive) or the absence of shock (learned safety). As mice likely generalize expected negative prediction from a previous aversive experience to learn relative aversive value or safety, our results are reminiscent of previous reports showing that the omission of expected reward activates the aPVT, but not the pPVT. [76] The aPVT may therefore be strongly involved in generating predictive value signals crucial for the encoding of relative aversive/safety values requiring the reward system. To compute these predictive value signals, the PVT receives inputs from regions such as the infralimbic, prelimbic cortex [27,85–88] and ventral hippocampus [89,90], which convey information about motivational state and arousal, respectively. To modulate predictive value signals, the PVT projects to the ventral tegmental area (VTA) and substantia nigra pars compacta [91] where computation of prediction error (comparison between predicted and actual information) is crucial to signal correct value to sensory experience during learning.[92,93] Notably, VTA dopaminergic neurons can regulate the salience of threat signals. [94] As the reward system is involved in both relative aversive value [6,7] and learned safety [14,16,17,95], the aPVT could modulate the computation of a relative positive value signals in the VTA. The aPVT also projects to regions modulating approach-avoidance behaviors such as prefrontal cortex [33,96] and ventral subiculum [96], extended amygdala [96,97], nucleus accumbens (NAc) shell [26,96,98] and NAc core. Since the NAc shell region integrates dopaminergic inputs from the VTA and (indirect) glutamatergic inputs from the PVT [99,100], inactivating the PVT-NAc pathway originating from aPVT D2+ neurons [101] could attenuate dopaminergic release in the NAc. Dopamine in the NAc is increased in response to safety cues[14], and recent work reveals that the PVT is required for this dopaminergic safety signal. [102]

408 Inactivating the aPVT D2+ neurons could lead to an aberrant assignment of value to neutral stimuli [103]
409 and therefore disrupt the ability to learn relative aversive and safety values. Unlike the pPVT, the aPVT
410 also receives major hippocampal subiculum projections. [27] During the relative comparison of
411 (aversive/safe) experiences, contextual information from the subiculum could be instrumental for the
412 generalization of threat prediction that aPVT D2+ neurons use to modulate reward VTA and/or NAc
413 circuits to enable the encoding of relative aversive/safe value.
414 Unlike innate safety towards a novel "naïve" CS, learned safety involves the discrimination between
415 CSs to avoid overgeneralization of a threat. Although several behavioral paradigms have been
416 developed to examine learned safety [14], most of the literature has focused on tasks where the animals
417 tested cannot escape a potentially dangerous situation, thereby restricting their repertoire of fear related
418 behaviors. This has led to safety been classically measured through freezing behavior [42,104,105].
419 However, paradigms beyond instrumental tasks [106,107] can incorporate safety approaching
420 measurements, and future studies should include measurements of safety such as the active approach
421 of a safe compartment as seen in conditioned place preference/avoidance paradigms such as ours.
422 Furthermore, our results revealed a preferential activation of aPVT D2+ neurons during learning relative
423 aversive value or safety, while paradoxically we and others found that D2+ neurons are preferentially
424 located in the pPVT. [33,49] Importantly, generalized threat prediction, involved here for learning relative
425 aversive value or learned safety, also involve the activation of D2 type receptors in the extended
426 amygdala substructures i.e., the central amygdala and the bed nucleus of the stria terminalis that have
427 been shown to contribute to anxiety-like behaviors. [108] Of note, aPVT D2+ neuronal activation was
428 tightly linked with the time spent in the bridge during choice test, a crucial behavioral hallmark of the
429 decision-making process between different options. Indeed, the less recruited aPVT D2+ neurons, but
430 not pPVT, the more animals spent time in the bridge in the relative aversive, but not safe, condition.
431 Consistent with this observation, we found that the selective inactivation of aPVT D2+ neurons
432 increased the time spent in the bridge in the relatively aversive, but not the safe, condition thus
433 preventing mice from selecting the most appropriate behavior when facing a complex decision between
434 two aversive situations.
435
436 **aPVT D2+ neuronal modulation of salience vs behavioral disinhibition**

437 Emotionally salient events, regardless whether positive or negative, are encoded and remembered with
438 greater accuracy compared to emotionally neutral ones. [109–113] The PVT is involved in arousal [33,114,115]
439 and can encode salience of both conditioned and unconditioned stimuli. [28] Prior work revealed the
440 existence of two subpopulations of PVT neurons that form molecularly, anatomically and functionally
441 distinct subpopulations. [33,49] For instance, D2+ neurons (type I neurons) send projections to the
442 prelimbic cortex and are sensitive to aversive stimuli. [33,39] By contrast, D2- neurons (type II neurons)
443 send projections to the infralimbic cortex and are modulated by stimulus salience. [33] However, given
444 the preferential anatomical distribution of D2+ neurons in the pPVT [33,35,49,101], most studies neglected
445 the contribution of D2+ neurons located in the aPVT. Further studies will therefore be required to
446 disentangle the role of the projections originating from D2+ or D2- neurons of the aPVT (targeting the
447 amygdala or NAc [33]). In this sense, our work not only sheds light on the role of aPVT D2+ neurons but
448 also, highlights, more broadly, the profound influence that even a relatively small neuronal population
449 can exert on relative value-based learning.
450 Our results showed that the inactivation of aPVT D2+, but not D2-, neurons enhances the relative
451 aversiveness or safeness of the ongoing experience, possibly by increasing its salience. Yet, it remains
452 unclear whether the conditioned stimulus (here, the context) or the outcome (shock or no shock
453 delivered) become more salient. In line with the latter option, such manipulation for the relative aversive
454 task increased tail rattling behavior immediately after the shock delivery during conditioning, but not
455 general freezing. Consistently, a recent study identified that tail rattling, but not freezing, behavior
456 positively scales with arousal level. [43] However, the precise neural mechanisms through which aPVT
457 neurons contribute to the expression of active defensive behavior such as tail rattling remain to be
458 defined. Inactivation of aPVT D2+ neurons also increased the number of turnbacks and time in the
459 bridge zone (i.e., hesitation) during the choice test, thus leading to the absence of preference for the
460 less punished context. Importantly, the same inactivation procedure during the safe conditioning did not
461 affect tail rattling behavior nor the time in the bridge zone, but it led to an increased preference for the
462 safe context. The efficiency of the value-based choices could therefore be influenced by the salience
463 of the experience and the computation and comparison of values assigned at the time of learning. [18]
464 Inactivation of aPVT D2+ neurons could have led to an incorrect value assignment during the context-
465 outcome association, thus favoring the contribution of D2- neurons for the attribution of salience to the
466 ongoing experience. [33,82] This could hamper (for the relative aversive task) or favor (for learned safety)

467 the ability of animals to distinguish between the options associated with each context. Inactivating aPVT
468 D2+ neurons could therefore enhance the formation of memory of any otherwise low-salient stimuli. An
469 alternative explanation could be that aPVT D2+ neurons provide a specific function in behavioral
470 disinhibition. [48,76,116–119] Then, inactivation of aPVT D2+ neurons during conditioning S2 could unleash
471 context-dependent behavior such as active defensive (tail rattling) behavior during relative comparison
472 of aversive experiences or decreased freezing and increased preference for the safe context. Indeed,
473 aPVT D2+ neurons could exert context-dependent behavioral disinhibition by modulating the salience
474 of contextual cues/information, which allows mice to detect the aversiveness or safeness of an
475 experience to disinhibit specific and adapted behaviors. However, testing these hypotheses will require
476 further investigation.
477 Unlike the opposite effect observed with D2+ neuronal inhibition over relative safety and aversive value
478 learning, D2- neurons seem to be engaged (increased cFos expression) in a similar manner
479 independently of whether the animal is comparing between two aversive experiences or an aversive
480 and a neutral one. Beas et al 2024 found a decreased activity of aPVT D2- neurons as animals
481 approach a reward.[120] Thus, inhibiting aPVT D2- neurons in our tasks may have transiently reduced
482 generalized fear expression (i.e., decreased freezing to contextual cues) without affecting the mouse's
483 ability to learn relative aversive/safety value.
484 Overall, our findings extend current knowledge about the role of PVT as an integrator of emotional,
485 contextual and sensory information to guide appropriate behavior. This study provides new evidence
486 regarding the role of aPVT D2+ neurons for contextual relative aversive/safety learning that supports
487 appropriate value-based decisions. A better understanding of the neuronal circuits and mechanisms
488 responsible for the balance between value information, salience and behavioral disinhibition is therefore
489 critical for deciphering motivated behaviors. Indeed, an excessive stimulus evaluation and/or salience
490 processing during traumatic events (that could involve the PVT) might lead to associative learning
491 impairment and contribute to the genesis of anxiety disorders such as PTSD. [121,122]
492
493 **Resource availability**
494 Further information and requests for resources and reagents should be directed to, and will be fulfilled
495 by, the corresponding authors, Emmanuel Perisse (emmanuel.perisse@igf.cnrs.fr) and Stéphanie
496 Trouche (stephanie.trouche@igf.cnrs.fr).

497

498 **Materials availability**

499 All original reagents presented in this study are available from the Lead Contacts upon request.

500

501 **Data and code availability**

502 All code used in this paper using Fiji will be shared by the Lead Contacts upon request.

503

504 **Methods**

505 **Animals**

506 We used C57BL/6J (Charles River Laboratories, France) and three transgenic heterozygous adult male
507 mouse lines: D2 Cre mice (STOCK Tg(*Drd2* cre) ER44Gsat/Mmucd, provided by E. Valjent), D2
508 Cre:Ribotag mice [123] (provided by E. Valjent) and D2 Cre:Ai14 mice, that were generated by crossing
509 Drd2 Cre mice with Ai14 mice (B6.Cg-*Gt(ROSA)26Sor*$^{tm14(CAG\text{-}tdTomato)Hze}$/J, stock #007914). The latter
510 transgenic mouse line expressed the red fluorescent protein double-tomato (tdTom) under endogenous
511 regulatory elements of the D2 receptor. All transgenic mice were maintained on a C57BL/6J
512 background. Animals (3 to 5-month-old mice) were housed with their littermates and were singly housed
513 in their home cage after the surgical procedure on a 12-h light/dark cycle (7 a.m. to 7 p.m.) in stable
514 temperature (22°C) and humidity (60%) conditions with free access to food and water in a dedicated
515 housing room. Mice were randomly assigned to behavioral groups. All experimental procedures were
516 conducted in agreement with the guidelines of the French Agriculture and Forestry Ministry for handling
517 animals (authorization number/license A3417241) and approved by the local and national ethic
518 committees (authorizations APAFIS #23355).

519

520 **Immunofluorescent staining and c-Fos analysis**

521 Mice (D2 Cre:Ai14 or D2 Cre:Ribotag, see **Figures 3** and **S3**) were anaesthetized and transcardially
522 perfused with PBS followed by 4% PFA in PBS solution 90 min after the second session of conditioning
523 of the CPP task. Brains were extracted and kept in 4% PFA for at least 24 h before slicing using the
524 vibratome and coronal sections (30µm thick) were stored in PBS-azide at 4°C. For the
525 immunohistochemistry procedures, free-floating sections were rinsed extensively in PBS with 0.25%
526 Triton X-100 (PBS-T) and blocked for 1 h at room temperature in PBS-T with 10% normal donkey serum

527 (NDS). An average of 3.5 sections per animal of either aPVT or pPVT were used. Sections were then
528 incubated overnight at room temperature with primary antibodies diluted in 3% NDS blocking solution.
529 The primary antibodies used were: anti-RFP (MBL, rabbit, 1/2000, #PM005), *c-Fos* antibody (Synaptic
530 Systems, rat, 1/5000, #226017), anti-HA (rabbit, 1/500, Rockland #600-401-384) and anti-GFP
531 (chicken, 1/2000, #GFP-1010). After three 15 min washes using PBS, sections were incubated for 2h30
532 at room temperature in PBS containing a mixture of secondary antibodies. Secondary antibodies used
533 were: donkey 488-coupled anti-rabbit (Jackson Laboratory, 1/500, #711-545-152), donkey Cy3-coupled
534 anti-rabbit (Jackson Laboratory, 1/1000, #711-165-152), donkey Cy5-coupled anti-rat (Jackson
535 Laboratory, 1/500, #712-605-150), donkey 488-coupled anti-rat (Jackson Laboratory, 1/500, #712-545-
536 153) and donkey Cy3-coupled anti-rat (Jackson Laboratory, 1/1000, #712-165-153). After three 15 min
537 washes in PBS, sections were mounted on slides and stored at 4°C. Images were taken using a ZEISS
538 Apotome microscope at 16bits and either 10X or 20X. cFos expression was examined in D2 tagged
539 cells using the D2 Cre:ai14 mice or D2 Cre:Ribotag (in a balanced manner by group) using ImageJ
540 based automated analysis. For each section, a region of interest was assigned for both aPVT and pPVT
541 and a threshold was selected to count both the amount of c-Fos+ cells, D2+ cells and c-Fos+ D2+
542 colocalization. Sections from aPVT were taken at AP:-0.22 to -1.22 while the pPVT were taken at AP:-
543 1.34 to -2.18.
544
545 ***In vivo* pharmacogenetic inhibition**
546 For *in vivo* pharmacogenetic (Designer Receptors Exclusively Activated by Designer Drugs, DREADD),
547 inhibition in CPP and contextual fear conditioning (CFC) experiments, Clozapine N-Oxide (2 mg/kg
548 CNO, Enzo Life Science, #BML-NS105-0025) was dissolved in 0.9% NaCl saline solution and
549 intraperitoneally (i.p.) injected 30 min before the conditioning session (for CFC) or the second
550 conditioning session (for CPP).
551
552 **Stereotaxic viral injections**
553 The following adeno-associated viral vectors (AAV) were used: AAV2/1-hSyn-DIO-hM4D(Gi)-mCherry,
554 (hM4Di, 7.1E12 vg/mL, #44362 Addgene), AAV2/1-hsyn-DIO-mCherry (control, 1.7E13 vg/mL, #50459
555 Addgene), AAV2/9-hSyn-FLEx-OFF-hM4D(Gi)-mCherry (hM4Di, 1.1E14 vg/mL, Plasmid #161579
556 Addgene), AAV2/9-hSyn-FLEx-OFF-mCherry (control, 6.1E14 vg/mL, designed in house from Plasmid

557 #161579 Addgene), AAV2/9-hSyn-FLEx-OFF-hM4D(Gi)-mCitrine (hM4Di, 1.8E15 vg/mL, designed in
558 house from Plasmid #161579 Addgene), AAV2/9-hSyn-FLEx-OFF-mCitrine (control, 1.9E15 vg/mL,
559 designed in house from Plasmid #161579 Addgene). Mice were anaesthetized with isoflurane (0.5–
560 3.5% oxygen gas mixture 1 l/min) and buprenorphine (0.1mg per kg of body weight) for stereotaxic
561 injections. Viral injections were targeted unilaterally to aPVT (coordinates: AP -0.40 mm; ML -0.60 mm;
562 DV -3.25 mm, 10° angle; 200 nl per site). The viral vectors were delivered at a rate of 100nl/min using
563 a glass micropipette lowered to the target site and that remained for 5 min after injection before it was
564 withdrawn. Mice were tested for behavior 4-5 weeks after viral injections. At least 7 days before testing,
565 animals were singled caged to prepare them for the behavioral experiment and trained with mock i.p.
566 injection.
567
568 **Behavioral procedures**
569 *Conditioned Place Preference experiments.*
570 We developed a 1-day aversive task based on a previously published conditioned place preference
571 (CPP) task. [46,47] The apparatus contained two electric grids on the floor of each context and consists of
572 two square-walled (46 cm × 46 cm × 30 cm) contexts with distinct inside building block configurations.
573 The two contexts were connected via a bridge (8-cm length, 7-cm width, 30cm height) during both
574 pretest and test sessions. The access to the bridge was blocked during each conditioning session. All
575 mice were handled for at least 3 days before the first experiment and, when experiments involved viral
576 injections, habituated to the injection procedure by mock injections during these days.
577 During pretest, mice freely explored the two distinct contexts (e.g. one square and one circle) for 15
578 min and their baseline (spontaneous) preference for one of the two contexts was determined. Next,
579 mice were subjected to a first 10 min-conditioning session (S1), in either no shock (0 mA, "A+0") or 4
580 shocks (0.6 mA or 0.3 mA of intensity, at 198 s, 278 s, 358 s and 438 s, 2-s duration each, as in [124])
581 were delivered in their most preferred context (Context A, "A+0.6" or "A+0.3"). Mice returned to their
582 home cage at the end of session S1 for 30 min. During the second 10 min-conditioning session S2,
583 mice received, in their least preferred enclosure (Context B), either no shock (0 mA, "B+0") or 4 shocks
584 (of 0.6 mA for "B+0.6" or 0.3 mA for "B+0.3" at 198 s, 278 s, 358 s and 438 s, of 2-s duration each).
585 The control group (0 vs 0) went through the two sessions S1 and S2 without receiving any shock. During
586 the choice-test session 1 hour later without any shock delivered, mice were placed in their most

587 preferred context A (as defined during pretest) and were free to visit the two enclosures for 15 min after
588 their first cross from context A to context B. For **Figure S4 P-T**, the mouse was placed in the non-
589 preferred (punished) context D during the choice test, and was free to visit the two enclosures for 15
590 min after their first cross from context D to context C. Mice that displayed more than 75% preference
591 during pretest were excluded for the rest of the procedure.
592
593 *Contextual fear conditioning experiments.*
594 A separated group of mice shown in **Figure 4** was subjected to classical contextual fear conditioning.
595 During the 10 min-conditioning session (S1), mice received 4 shocks of 0.3 mA each in Context B
596 ("B+0.3" at 198 s, 278 s, 358 s and 438 s, of 2-s duration each). All mice were tested in the same
597 context 1h later without any shock delivered for 15min (retrieval test session).
598
599 *Behavioral analysis*
600 Mice were tracked and several behavioral parameters were measured during pretest, conditioning and
601 choice test. A conditioned place preference score (CPP score) was calculated for each mouse during
602 both pretest and choice test as in [47]. Mice that did not cross to the non-preferred context B in less than
603 25 min were excluded from further analysis (i.e. they did not perform the following 15 min choice test).
604 CPP was calculated as $CPP = \frac{t_{non\,preferred} - t_{preferred}}{t_{non\,preferred} + t_{preferred}}$. ΔCPP was calculated as the difference between
605 CPP test and CPP pretest. The first latency to cross was the time the animal takes to first cross from
606 the originally preferred context A (where they were first placed) to the originally non-preferred context
607 B. The second latency to cross was the time the animal takes to cross back to the preferred context A.
608 Time in the bridge was measured during the first latency (time in the bridge before first cross) and during
609 the first 5 min after the first cross. Freezing behavior was systematically measured using a custom-
610 made software (Imetronic) and was calculated as the percentage of time for which mice remained
611 immobile for 2 s or more. The percentage of time spent freezing during the entire duration of the pretest
612 and test session were reported. For each conditioning session, the percentage of freezing before the
613 1st shock (min 1-3) and after the 4th shock (min 9-10) were calculated. For **Figure 1B**, the difference
614 between the total percentage of freezing in S2 minus the total percentage of freezing in S1 was
615 calculated for each group (total percentage of freezing for S1 and S2 used for this calculation are
616 presented in **Figure S1**). All relative measurements (ΔCPP, ΔTime in bridge, etc) were calculated by

617 subtracting choice test behavioral measurements with the corresponding measurement during the
618 pretest. For example, ΔTime in the bridge was calculated as the time spent in the bridge during the first
619 5 min after crossing during the choice test minus the time spent in the bridge during the first 5 min of
620 the pretest session, ie. $\Delta Time\ bridge = Time\ bridge\ Choice_{0-5min} - Time\ bridge\ Pretest_{0-5min}$. We
621 quantified whether the animal engaged in turn back behavior (i.e. when the whole body turns at 180
622 degree) before 1st crossing from A to B when the animal was in the bridge. Tail rattling was measured
623 as a rapid vibration of the tail either after each shock delivered during conditioning sessions S1 and S2
624 or before the first cross during the choice test. For experiments shown in **Figure S4**, animals from the
625 0-0.3 condition were animals that went through CFC one week before. A different set of contexts (C
626 and D) with electric grids. For experiments shown in **Figure S7**, animals from the 0-0 control group
627 were animals that went through the 0.3-0.3 condition one week before. A different set of contexts (C
628 and D) were used in which the floor was plain and without grids. For measuring the distance travelled
629 post shock delivery as done in [125], we averaged for each conditioning session the distance travelled for
630 8 sec at the onset of each shock event (i.e. 198-206 s, 278-286 s, 358-366 s, 438-446 s).
631 In **Figure 5**, 1 mCherry animal was excluded for not crossing during choice test, 2 hM4Di and 1 mCherry
632 animals were excluded for transduced cells found outside PVT. In **Figure 6**, 1 hM4Di and 1 mCherry
633 animal were excluded for not crossing during choice test. In **Figure 7**, 1 hM4Di animal was excluded
634 for transduced cells found outside PVT.
635
636 **Brain slice electrophysiology**
637 Patch-clamp recordings, in whole-cell configuration, were performed on PVT D2-labeled cells in current
638 clamp mode. Briefly, injected D2 Cre mice (n=4 for Cre ON condition and n=4 for Cre OFF condition;
639 for each condition, 2 mCherry and 2 hM4Di mice) were anesthetized and perfused intracardially with
640 ice-cold dissection buffer (25 mM NaHCO3, 1.25 mM, NaH2PO4, 2.5 mM KCl, 0.5 mM CaCL2, 7 mM
641 MgCl2, 25 mM D-glucose, 110 mM choline chloride, 11.6 mM ascorbic acid, 3.1 mM Pyruvic acid
642 maintained in 5% CO2/ 95% O2). Coronal brain slices (350 µm) were cut in dissection buffer using a
643 vibratome (Campden Instruments). Sections were incubated in artificial cerebrospinal fluid (ACSF)
644 containing the following (in mM) 125 NaCl, 2.7 KCl, 11.6 NaHCO3, 0.4 NaH2PO4, 1 MgCl2, 2 CaCl2,
645 5.6 D-glucose (pH 7.4, osmolarity 305 mOsm) at 32°C for 5 min and then kept in room temperature for
646 at least 1h before recording. For the experiment, slices were superfused continuously at 1.5 ml/min with

647 an ACSF solution. Recordings were obtained using a Multiclamp 700B amplifier (Molecular Devices).
648 Recording electrodes made of borosilicate glass had a resistance of 4-6 MΩ (Warner Instruments, USA)
649 and were filled with K-gluconate solution containing (in mM) 125 K-gluconate, 5 KCl, 10 Hepes, 1 EGTA,
650 5 Na-phosphocreatine, 0.07 CaCl2, 2 Mg-ATP, 0.4 Na-GTP (pH 7.2, osmolarity 300 mOsm). Only cells
651 with access resistance < 20 MΩ and a change of resistance < 25% over the course of the experiment
652 were analyzed. Data were filtered with a Hum Bug (Quest Scientific, Canada), digitized at 2 kHz
653 (Digidata 1444A, Molecular Devices, Sunnyvale, CA, USA), and acquired using Clampex 10 software
654 (Molecular Devices). Whole cell recordings were made from mCherry aPVT D2+ or D2- neurons
655 visualized with an Olympus microscope (equipped with an mCherry filter). CNO was dissolved in ACSF
656 (10μM, 300 s) and applied in the bath after 5 min baseline recording. The number of action potentials
657 were analyzed before and after CNO application with Clampfit 10 software (Axon Instruments).
658
659 **Statistical Analysis**
660 Data were shown as the mean ± SEM (standard error of the mean). GraphPad Prism v10 software was
661 used for statistical analyses. D'Agostino-Pearson omnibus test is used as a test for normality. When
662 this assumption was not met, non-parametric tests were used (see **Table S1**). Student's t-test (paired
663 or unpaired, 2-sided) was used to compare two sets of data. Multiple comparisons were performed by
664 1-way or 2-way ANOVA followed by either Sidak's, Tukey's, Uncorrected Fisher's LSD or Dunn's
665 multiple comparisons were used for *post-hoc* analysis. For comparisons against 0, either one sample t
666 test or Wilcoxon signed rank test (for non-normal data) were used. All statistical comparisons are
667 presented in **Table S1**.
668
669 **Acknowledgements**
670 We warmly thank S. Parkes and G. Gangarossa for their valuable comments on the manuscript. We
671 thank M. Verdy for his help with setting up the behavioral task. We thank the vector core facility of
672 Montpellier /Plateforme de Vectorologie de Montpellier, BioCampus, UM-CNRS-INSERM, Montpellier,
673 France, especially C.Lemmers for producing the Cre Off viruses. We thank E. Valjent for sharing the
674 D2 Cre mouse line. This work was supported by CNRS, INSERM, the IGF, the ATIP-Avenir program
675 (EP), the Bettencourt Schueller Foundation (EP), the French Research Agency (ANR-19-CE37-0006,
676 ST and LV; ANR-21-CE16-0015, EP, ST, MD and EK), the CBS2 doctoral school of Montpellier (EK),

the Human Frontier Science Program Postdoctoral Fellowship (LT0027-2022-L, MM) and Fyssen Foundation (MM). We acknowledge the imaging facility MRI, member of the France-BioImaging national infrastructure supported by the French National Research Agency (ANR-10-INBS-04, “Investments for the future”). We also thank all the Iexplore staff from IGF, especially M. Dedin, for their help in the maintenance and breeding of mice.

AUTHOR CONTRIBUTIONS

M.M., E.P. and S.T. conceived the project and designed all the experiments. M.M. and E.K. performed surgical and anatomical experiments. M.M., E.K., L.V., M.D and C.V. performed behavioral experiments. P.T., M.P, E.K. and J.S. performed and analyzed electrophysiological experiments. M.L. and E.K. helped with cloning constructs and viral strategies. The manuscript was written by M.M., E.P. and S.T and commented by all authors. All authors were asked for input on the text.

DECLARATION OF INTERESTS

The authors declare no competing interests.

REFERENCES

1. Rumbaugh, D.M., King, J.E., Beran, M.J., Washburn, D.A., and Gould, K.L. (2007). A Salience Theory of Learning and Behavior: With Perspectives on Neurobiology and Cognition. Int J Primatol *28*, 973–996. https://doi.org/10.1007/s10764-007-9179-8.

2. Domjan, M. (2005). Pavlovian conditioning: a functional perspective. Annu Rev Psychol *56*, 179–206. https://doi.org/10.1146/annurev.psych.55.090902.141409.

3. Rangel, A., Camerer, C., and Montague, P.R. (2008). A framework for studying the neurobiology of value-based decision making. Nat. Rev. Neurosci. *9*, 545–556. https://doi.org/10.1038/nrn2357.

4. Dunsmoor, J.E., and Paz, R. (2015). Fear Generalization and Anxiety: Behavioral and Neural Mechanisms. Biological Psychiatry *78*, 336–343. https://doi.org/10.1016/j.biopsych.2015.04.010.

5. Kobayashi, S., and Schultz, W. (2014). Reward Contexts Extend Dopamine Signals to Unrewarded Stimuli. Curr Biol *24*, 56–62. https://doi.org/10.1016/j.cub.2013.10.061.

6. Brooks, A.M., Pammi, V.S.C., Noussair, C., Capra, C.M., Engelmann, J.B., and Berns, G.S. (2010). From Bad to Worse: Striatal Coding of the Relative Value of Painful Decisions. Front Neurosci *4*. https://doi.org/10.3389/fnins.2010.00176.

7. Villar, M.E., Pavão-Delgado, M., Amigo, M., Jacob, P.F., Merabet, N., Pinot, A., Perry, S.A., Waddell, S., and Perisse, E. (2022). Differential coding of absolute and relative aversive value in the Drosophila brain. Current Biology *32*, 4576-4592.e5. https://doi.org/10.1016/j.cub.2022.08.058.

711 8. Diederen, K.M.J., Ziauddeen, H., Vestergaard, M.D., Spencer, T., Schultz, W., and Fletcher, P.C.
712 (2017). Dopamine Modulates Adaptive Prediction Error Coding in the Human Midbrain and
713 Striatum. J Neurosci *37*, 1708–1720. https://doi.org/10.1523/JNEUROSCI.1979-16.2016.

714 9. Saez, R.A., Saez, A., Paton, J.J., Lau, B., and Salzman, C.D. (2017). Distinct roles for the
715 amygdala and orbitofrontal cortex in representing the relative amount of expected reward. Neuron
716 *95*, 70-77.e3. https://doi.org/10.1016/j.neuron.2017.06.012.

717 10. Seymour, B., and McClure, S.M. (2008). Anchors, scales and the relative coding of value in
718 the brain. Curr. Opin. Neurobiol. *18*, 173–178. https://doi.org/10.1016/j.conb.2008.07.010.

719 11. Tremblay, L., and Schultz, W. (1999). Relative reward preference in primate orbitofrontal
720 cortex. Nature *398*, 704–708. https://doi.org/10.1038/19525.

721 12. Antoniadis, E.A., and McDonald, R.J. (2000). Amygdala, hippocampus and discriminative fear
722 conditioning to context. Behavioural Brain Research *108*, 1–19. https://doi.org/10.1016/S0166-
723 4328(99)00121-7.

724 13. Sangha, S., Diehl, M.M., Bergstrom, H.C., and Drew, M.R. (2020). Know Safety, No Fear.
725 Neurosci Biobehav Rev *108*, 218–230. https://doi.org/10.1016/j.neubiorev.2019.11.006.

726 14. Duvarci, S. (2024). Dopaminergic circuits controlling threat and safety learning. Trends in
727 Neurosciences *47*, 1014–1027. https://doi.org/10.1016/j.tins.2024.10.001.

728 15. Perisse, E., Yin, Y., Lin, A.C., Lin, S., Huetteroth, W., and Waddell, S. (2013). Different
729 Kenyon Cell Populations Drive Learned Approach and Avoidance in Drosophila. Neuron *79*, 945–
730 956. https://doi.org/10.1016/j.neuron.2013.07.045.

731 16. Rogan, M.T., Leon, K.S., Perez, D.L., and Kandel, E.R. (2005). Distinct Neural Signatures for
732 Safety and Danger in the Amygdala and Striatum of the Mouse. Neuron *46*, 309–320.
733 https://doi.org/10.1016/j.neuron.2005.02.017.

734 17. Jacob, P.F., and Waddell, S. (2020). Spaced Training Forms Complementary Long-Term
735 Memories of Opposite Valence in Drosophila. Neuron *106*, 977-991.e4.
736 https://doi.org/10.1016/j.neuron.2020.03.013.

737 18. Hunter, L.E., and Daw, N.D. (2021). Context-sensitive valuation and learning. Current Opinion
738 in Behavioral Sciences *41*, 122–127. https://doi.org/10.1016/j.cobeha.2021.05.001.

739 19. Zweifel, L.S. (2019). Dopamine, uncertainty, and fear generalization. Current Opinion in
740 Behavioral Sciences *26*, 157–164. https://doi.org/10.1016/j.cobeha.2019.01.003.

741 20. Nasser, H.M., and McNally, G.P. (2012). Appetitive–aversive interactions in Pavlovian fear
742 conditioning. Behavioral Neuroscience *126*, 404–422. https://doi.org/10.1037/a0028341.

743 21. Felsenberg, J., Jacob, P.F., Walker, T., Barnstedt, O., Edmondson-Stait, A.J., Pleijzier, M.W.,
744 Otto, N., Schlegel, P., Sharifi, N., Perisse, E., et al. (2018). Integration of Parallel Opposing
745 Memories Underlies Memory Extinction. Cell *175*, 709-722.e15.
746 https://doi.org/10.1016/j.cell.2018.08.021.

747 22. Zhang, X., Kim, J., and Tonegawa, S. (2020). Amygdala Reward Neurons Form and Store
748 Fear Extinction Memory. Neuron *105*, 1077-1093.e7. https://doi.org/10.1016/j.neuron.2019.12.025.

749 23. Kirouac, G.J. (2015). Placing the paraventricular nucleus of the thalamus within the brain
750 circuits that control behavior. Neuroscience & Biobehavioral Reviews *56*, 315–329.
751 https://doi.org/10.1016/j.neubiorev.2015.08.005.

752 24. Kirouac, G.J. (2021). The Paraventricular Nucleus of the Thalamus as an Integrating and
753 Relay Node in the Brain Anxiety Network. Front. Behav. Neurosci. *15*.
754 https://doi.org/10.3389/fnbeh.2021.627633.

25. Moga, M.M., Weis, R.P., and Moore, R.Y. (1995). Efferent projections of the paraventricular thalamic nucleus in the rat. J Comp Neurol *359*, 221–238. https://doi.org/10.1002/cne.903590204.

26. Vertes, R.P., and Hoover, W.B. (2008). Projections of the paraventricular and paratenial nuclei of the dorsal midline thalamus in the rat. Journal of Comparative Neurology *508*, 212–237. https://doi.org/10.1002/cne.21679.

27. Li, S., and Kirouac, G.J. (2012). Sources of inputs to the anterior and posterior aspects of the paraventricular nucleus of the thalamus. Brain Struct Funct *217*, 257–273. https://doi.org/10.1007/s00429-011-0360-7.

28. Zhu, Y., Nachtrab, G., Keyes, P.C., Allen, W.E., Luo, L., and Chen, X. (2018). Dynamic Salience Processing in Paraventricular Thalamus Gates Associative Learning. Science *362*, 423–429. https://doi.org/10.1126/science.aat0481.

29. Garau, C., Liu, X., Calo, G., Schulz, S., and Reinscheid, R.K. (2022). Neuropeptide S Encodes Stimulus Salience in the Paraventricular Thalamus. Neuroscience *496*, 83–95. https://doi.org/10.1016/j.neuroscience.2022.06.013.

30. Haight, J.L., Fraser, K.M., Akil, H., and Flagel, S.B. (2015). Lesions of the paraventricular nucleus of the thalamus differentially affect sign- and goal-tracking conditioned responses. European Journal of Neuroscience *42*, 2478–2488. https://doi.org/10.1111/ejn.13031.

31. Haight, J.L., Campus, P., Maria-Rios, C.E., Johnson, A.M., Klumpner, M.S., Kuhn, B.N., Covelo, I.R., Morrow, J.D., and Flagel, S.B. (2020). The lateral hypothalamus and orexinergic transmission in the paraventricular thalamus promote the attribution of incentive salience to reward-associated cues. Psychopharmacology (Berl) *237*, 3741–3758. https://doi.org/10.1007/s00213-020-05651-4.

32. Campus, P., Covelo, I.R., Kim, Y., Parsegian, A., Kuhn, B.N., Lopez, S.A., Neumaier, J.F., Ferguson, S.M., Solberg Woods, L.C., Sarter, M., et al. (2019). The paraventricular thalamus is a critical mediator of top-down control of cue-motivated behavior in rats. eLife *8*, e49041. https://doi.org/10.7554/eLife.49041.

33. Gao, C., Leng, Y., Ma, J., Rooke, V., Rodriguez-Gonzalez, S., Ramakrishnan, C., Deisseroth, K., and Penzo, M.A. (2020). Two genetically, anatomically and functionally distinct cell types segregate across anteroposterior axis of paraventricular thalamus. Nat Neurosci *23*, 217–228. https://doi.org/10.1038/s41593-019-0572-3.

34. Perisse, E., Miranda, M., and Trouche, S. (2023). Modulation of aversive value coding in the vertebrate and invertebrate brain. Current Opinion in Neurobiology *79*, 102696. https://doi.org/10.1016/j.conb.2023.102696.

35. Barson, J.R., Mack, N.R., and Gao, W.-J. (2020). The Paraventricular Nucleus of the Thalamus Is an Important Node in the Emotional Processing Network. Front. Behav. Neurosci. *14*. https://doi.org/10.3389/fnbeh.2020.598469.

36. Do-Monte, F.H., Quinones-Laracuente, K., and Quirk, G.J. (2015). A temporal shift in the circuits mediating retrieval of fear memory. Nature *519*, 460–463. https://doi.org/10.1038/nature14030.

37. Choi, E.A., Jean-Richard-dit-Bressel, P., Clifford, C.W.G., and McNally, G.P. (2019). Paraventricular Thalamus Controls Behavior during Motivational Conflict. J Neurosci *39*, 4945–4958. https://doi.org/10.1523/JNEUROSCI.2480-18.2019.

38. Penzo, M.A., Robert, V., Tucciarone, J., De Bundel, D., Wang, M., Van Aelst, L., Darvas, M., Parada, L.F., Palmiter, R., He, M., et al. (2015). The paraventricular thalamus controls a central amygdala fear circuit. Nature *519*, 455–459. https://doi.org/10.1038/nature13978.

39. Beas, B.S., Wright, B.J., Skirzewski, M., Leng, Y., Hyun, J.H., Koita, O., Ringelberg, N., Kwon, H.-B., Buonanno, A., and Penzo, M.A. (2018). The locus coeruleus drives disinhibition in the midline thalamus via a dopaminergic mechanism. Nat Neurosci *21*, 963–973. https://doi.org/10.1038/s41593-018-0167-4.

40. Li, Y., Dong, X., Li, S., and Kirouac, G.J. (2014). Lesions of the posterior paraventricular nucleus of the thalamus attenuate fear expression. Front. Behav. Neurosci. *8*. https://doi.org/10.3389/fnbeh.2014.00094.

41. Ma, J., du Hoffmann, J., Kindel, M., Beas, B.S., Chudasama, Y., and Penzo, M.A. (2021). Divergent projections of the paraventricular nucleus of the thalamus mediate the selection of passive and active defensive behaviors. Nat Neurosci *24*, 1429–1440. https://doi.org/10.1038/s41593-021-00912-7.

42. Wang, Z., Wang, Z., and Zhou, Q. (2024). Modulation of learning safety signals by acute stress: paraventricular thalamus and prefrontal inhibition. Neuropsychopharmacol. *49*, 961–973. https://doi.org/10.1038/s41386-023-01790-2.

43. Salay, L.D., Ishiko, N., and Huberman, A.D. (2018). A midline thalamic circuit determines reactions to visual threat. Nature *557*, 183. https://doi.org/10.1038/s41586-018-0078-2.

44. Tolman, E.C. (1939). Prediction of vicarious trial and error by means of the schematic sowbug. Psychological Review *46*, 318–336. https://doi.org/10.1037/h0057054.

45. Redish, A.D. (2016). Vicarious trial and error. Nat Rev Neurosci *17*, 147–159. https://doi.org/10.1038/nrn.2015.30.

46. Trouche, S., Perestenko, P.V., van de Ven, G.M., Bratley, C.T., McNamara, C.G., Campo-Urriza, N., Black, S.L., Reijmers, L.G., and Dupret, D. (2016). Recoding a cocaine-place memory engram to a neutral engram in the hippocampus. Nat. Neurosci. *19*, 564–567. https://doi.org/10.1038/nn.4250.

47. Trouche, S., Koren, V., Doig, N.M., Ellender, T.J., El-Gaby, M., Lopes-Dos-Santos, V., Reeve, H.M., Perestenko, P.V., Garas, F.N., Magill, P.J., et al. (2019). A Hippocampus-Accumbens Tripartite Neuronal Motif Guides Appetitive Memory in Space. Cell *176*, 1393-1406.e16. https://doi.org/10.1016/j.cell.2018.12.037.

48. Engelke, D.S., Zhang, X.O., O'Malley, J.J., Fernandez-Leon, J.A., Li, S., Kirouac, G.J., Beierlein, M., and Do-Monte, F.H. (2021). A hypothalamic-thalamostriatal circuit that controls approach-avoidance conflict in rats. Nat Commun *12*, 2517. https://doi.org/10.1038/s41467-021-22730-y.

49. Gao, C., Gohel, C.A., Leng, Y., Ma, J., Goldman, D., Levine, A.J., and Penzo, M.A. (2023). Molecular and spatial profiling of the paraventricular nucleus of the thalamus. eLife *12*, e81818. https://doi.org/10.7554/eLife.81818.

50. Rivera-Irizarry, J.K., Hámor, P.U., Rowson, S.A., Asfouri, J., Liu, D., Zallar, L.J., Garcia, A.F., Skelly, M.J., and Pleil, K.E. (2023). Valence and salience encoding by parallel circuits from the paraventricular thalamus to the nucleus accumbens. Preprint at bioRxiv, https://doi.org/10.1101/2023.07.03.547570 https://doi.org/10.1101/2023.07.03.547570.

51. Beier, K.T., Kim, C.K., Hoerbelt, P., Hung, L.W., Heifets, B.D., DeLoach, K.E., Mosca, T.J., Neuner, S., Deisseroth, K., Luo, L., et al. (2017). Rabies screen reveals GPe control of cocaine-triggered plasticity. Nature *549*, 345–350. https://doi.org/10.1038/nature23888.

52. Kong, M.-S., Ancell, E., Witten, D.M., and Zweifel, L.S. (2024). Valence and Salience Encoding in the Central Amygdala. Preprint, https://doi.org/10.1101/2024.07.05.602310 https://doi.org/10.1101/2024.07.05.602310.

845 53. Robinson, T., and Berridge, K. (2003). Addiction. Annual review of psychology *54*, 25–53.
846 https://doi.org/10.1146/annurev.psych.54.101601.145237.

847 54. Padoa-Schioppa, C., and Assad, J.A. (2006). Neurons in the orbitofrontal cortex encode
848 economic value. Nature *441*, 223–226. https://doi.org/10.1038/nature04676.

849 55. Hosokawa, T., Kato, K., Inoue, M., and Mikami, A. (2007). Neurons in the macaque
850 orbitofrontal cortex code relative preference of both rewarding and aversive outcomes. Neurosci.
851 Res. *57*, 434–445. https://doi.org/10.1016/j.neures.2006.12.003.

852 56. Matsumoto, M., and Hikosaka, O. (2009). How do dopamine neurons represent positive and
853 negative motivational events? Nature *459*, 837–841. https://doi.org/10.1038/nature08028.

854 57. Steinberg, E.E., Gore, F., Heifets, B.D., Taylor, M.D., Norville, Z.C., Beier, K.T., Földy, C.,
855 Lerner, T.N., Luo, L., Deisseroth, K., et al. (2020). Amygdala-Midbrain Connections Modulate
856 Appetitive and Aversive Learning. Neuron *106*, 1026-1043.e9.
857 https://doi.org/10.1016/j.neuron.2020.03.016.

858 58. Delgado, M.R., Li, J., Schiller, D., and Phelps, E.A. (2008). The role of the striatum in
859 aversive learning and aversive prediction errors. Philos Trans R Soc Lond B Biol Sci *363*, 3787–
860 3800. https://doi.org/10.1098/rstb.2008.0161.

861 59. Menegas, W., Akiti, K., Amo, R., Uchida, N., and Watabe-Uchida, M. (2018). Dopamine
862 neurons projecting to the posterior striatum reinforce avoidance of threatening stimuli. Nat
863 Neurosci *21*, 1421–1430. https://doi.org/10.1038/s41593-018-0222-1.

864 60. Kobayashi, K., Lee, S., Filipowicz, A.L.S., McGaughey, K.D., Kable, J.W., and Nassar, M.R.
865 (2021). Dynamic Representation of the Subjective Value of Information. J Neurosci *41*, 8220–
866 8232. https://doi.org/10.1523/JNEUROSCI.0423-21.2021.

867 61. Knutson, B., Adams, C.M., Fong, G.W., and Hommer, D. (2001). Anticipation of Increasing
868 Monetary Reward Selectively Recruits Nucleus Accumbens. J. Neurosci. *21*, RC159–RC159.
869 https://doi.org/10.1523/JNEUROSCI.21-16-j0002.2001.

870 62. McClure, S.M., Li, J., Tomlin, D., Cypert, K.S., Montague, L.M., and Montague, P.R. (2004).
871 Neural Correlates of Behavioral Preference for Culturally Familiar Drinks. Neuron *44*, 379–387.
872 https://doi.org/10.1016/j.neuron.2004.09.019.

873 63. Preuschoff, K., Bossaerts, P., and Quartz, S.R. (2006). Neural Differentiation of Expected
874 Reward and Risk in Human Subcortical Structures. Neuron *51*, 381–390.
875 https://doi.org/10.1016/j.neuron.2006.06.024.

876 64. Tobler, P.N., O'Doherty, J.P., Dolan, R.J., and Schultz, W. (2007). Reward Value Coding
877 Distinct From Risk Attitude-Related Uncertainty Coding in Human Reward Systems. J
878 Neurophysiol *97*, 1621–1632. https://doi.org/10.1152/jn.00745.2006.

879 65. Constantinople, C.M., Piet, A.T., Bibawi, P., Akrami, A., Kopec, C., and Brody, C.D. (2019).
880 Lateral orbitofrontal cortex promotes trial-by-trial learning of risky, but not spatial, biases. eLife *8*,
881 e49744. https://doi.org/10.7554/eLife.49744.

882 66. John, R.D.S. (1973). Genetic Analysis of Tail Rattling in the Mouse. Nature *241*, 549–551.
883 https://doi.org/10.1038/241549a0.

884 67. Choi, E.A., and McNally, G.P. (2017). Paraventricular Thalamus Balances Danger and
885 Reward. J. Neurosci. *37*, 3018–3029. https://doi.org/10.1523/JNEUROSCI.3320-16.2017.

886 68. Muenzinger, K.F. (1938). Vicarious Trial and Error at a Point of Choice: I. A General Survey
887 of its Relation to Learning Efficiency. The Pedagogical Seminary and Journal of Genetic
888 Psychology *53*, 75–86. https://doi.org/10.1080/08856559.1938.10533799.

69. Hu, D., and Amsel, A. (1995). A simple test of the vicarious trial-and-error hypothesis of hippocampal function. Proc Natl Acad Sci U S A *92*, 5506–5509.

70. Schmidt, B., Hinman, J.R., Jacobson, T.K., Szkudlarek, E., Argraves, M., Escabí, M.A., and Markus, E.J. (2013). Dissociation between Dorsal and Ventral Hippocampal Theta Oscillations during Decision-Making. J. Neurosci. *33*, 6212–6224. https://doi.org/10.1523/JNEUROSCI.2915-12.2013.

71. Steiner, A.P., and Redish, A.D. (2014). Behavioral and neurophysiological correlates of regret in rat decision-making on a neuroeconomic task. Nat Neurosci *17*, 995–1002. https://doi.org/10.1038/nn.3740.

72. Pliota, P., Böhm, V., Grössl, F., Griessner, J., Valenti, O., Kraitsy, K., Kaczanowska, J., Pasieka, M., Lendl, T., Deussing, J.M., et al. (2020). Stress peptides sensitize fear circuitry to promote passive coping. Mol Psychiatry *25*, 428–441. https://doi.org/10.1038/s41380-018-0089-2.

73. Zhu, Y., Wienecke, C.F.R., Nachtrab, G., and Chen, X. (2016). A thalamic input to the nucleus accumbens mediates opiate dependence. Nature *530*, 219–222. https://doi.org/10.1038/nature16954.

74. Zhu, Y.-B., Wang, Y., Hua, X.-X., Xu, L., Liu, M.-Z., Zhang, R., Liu, P.-F., Li, J.-B., Zhang, L., and Mu, D. PBN-PVT projections modulate negative affective states in mice. eLife *11*, e68372. https://doi.org/10.7554/eLife.68372.

75. Otis, J.M., Zhu, M., Namboodiri, V.M.K., Cook, C.A., Kosyk, O., Matan, A.M., Ying, R., Hashikawa, Y., Hashikawa, K., Trujillo-Pisanty, I., et al. (2019). Paraventricular Thalamus Projection Neurons Integrate Cortical and Hypothalamic Signals for Cue-Reward Processing. Neuron *103*, 423-431.e4. https://doi.org/10.1016/j.neuron.2019.05.018.

76. Do-Monte, F.H., Minier-Toribio, A., Quiñones-Laracuente, K., Medina-Colón, E.M., and Quirk, G.J. (2017). Thalamic Regulation of Sucrose Seeking during Unexpected Reward Omission. Neuron *94*, 388-400.e4. https://doi.org/10.1016/j.neuron.2017.03.036.

77. Hamlin, A.S., Clemens, K.J., Choi, E.A., and McNally, G.P. (2009). Paraventricular thalamus mediates context-induced reinstatement (renewal) of extinguished reward seeking. Eur J Neurosci *29*, 802–812. https://doi.org/10.1111/j.1460-9568.2009.06623.x.

78. Zhang, X., and van den Pol, A.N. (2017). Rapid binge-like eating and body weight gain driven by zona incerta GABA neuron activation. Science *356*, 853–859. https://doi.org/10.1126/science.aam7100.

79. Beck, C., and Fibiger, H. (1995). Conditioned fear-induced changes in behavior and in the expression of the immediate early gene c-fos: with and without diazepam pretreatment. J Neurosci *15*, 709–720. https://doi.org/10.1523/JNEUROSCI.15-01-00709.1995.

80. Yasoshima, Y., Scott, T.R., and Yamamoto, T. (2007). Differential activation of anterior and midline thalamic nuclei following retrieval of aversively motivated learning tasks. Neuroscience *146*, 922–930. https://doi.org/10.1016/j.neuroscience.2007.02.044.

81. Igelstrom, K.M., Herbison, A.E., and Hyland, B.I. (2010). Enhanced c-Fos expression in superior colliculus, paraventricular thalamus and septum during learning of cue-reward association. Neuroscience *168*, 706–714. https://doi.org/10.1016/j.neuroscience.2010.04.018.

82. Haight, J.L., and Flagel, S.B. (2014). A potential role for the paraventricular nucleus of the thalamus in mediating individual variation in Pavlovian conditioned responses. Front Behav Neurosci *8*. https://doi.org/10.3389/fnbeh.2014.00079.

83. Hsu, D.T., Kirouac, G.J., Zubieta, J.-K., and Bhatnagar, S. (2014). Contributions of the paraventricular thalamic nucleus in the regulation of stress, motivation, and mood. Front Behav Neurosci *8*, 73. https://doi.org/10.3389/fnbeh.2014.00073.

84. Matzeu, A., Weiss, F., and Martin-Fardon, R. (2015). Transient inactivation of the posterior paraventricular nucleus of the thalamus blocks cocaine-seeking behavior. Neurosci Lett *608*, 34–39. https://doi.org/10.1016/j.neulet.2015.10.016.

85. Sangha, S., Robinson, P.D., Greba, Q., Davies, D.A., and Howland, J.G. (2014). Alterations in Reward, Fear and Safety Cue Discrimination after Inactivation of the Rat Prelimbic and Infralimbic Cortices. Neuropsychopharmacology *39*, 2405–2413. https://doi.org/10.1038/npp.2014.89.

86. Tao, Y., Cai, C.-Y., Xian, J.-Y., Kou, X.-L., Lin, Y.-H., Qin, C., Wu, H.-Y., Chang, L., Luo, C.-X., and Zhu, D.-Y. (2020). Projections from Infralimbic Cortex to Paraventricular Thalamus Mediate Fear Extinction Retrieval. Neurosci Bull *37*, 229–241. https://doi.org/10.1007/s12264-020-00603-6.

87. Brown, A., and Chaudhri, N. (2023). Optogenetic stimulation of infralimbic cortex projections to the paraventricular thalamus attenuates context-induced renewal. European Journal of Neuroscience *57*, 762–779. https://doi.org/10.1111/ejn.15862.

88. Ng, K.H., and Sangha, S. (2022). Encoding of conditioned inhibitors of fear in the infralimbic cortex. Cereb Cortex *33*, 5658–5670. https://doi.org/10.1093/cercor/bhac450.

89. Li, S.H., Li, S., and Kirouac, G.J. (2024). Analysis of Monosynaptic Inputs to Thalamic Paraventricular Nucleus Neurons Innervating the Shell of the Nucleus Accumbens and Central Extended Amygdala. Neuroscience *537*, 151–164. https://doi.org/10.1016/j.neuroscience.2023.11.033.

90. Meyer, H.C., Odriozola, P., Cohodes, E.M., Mandell, J.D., Li, A., Yang, R., Hall, B.S., Haberman, J.T., Zacharek, S.J., Liston, C., et al. (2019). Ventral hippocampus interacts with prelimbic cortex during inhibition of threat response via learned safety in both mice and humans. Proceedings of the National Academy of Sciences *116*, 26970–26979. https://doi.org/10.1073/pnas.1910481116.

91. Watabe-Uchida, M., Zhu, L., Ogawa, S.K., Vamanrao, A., and Uchida, N. (2012). Whole-Brain Mapping of Direct Inputs to Midbrain Dopamine Neurons. Neuron *74*, 858–873. https://doi.org/10.1016/j.neuron.2012.03.017.

92. Glimcher, P.W. (2011). Understanding dopamine and reinforcement learning: The dopamine reward prediction error hypothesis. Proc Natl Acad Sci U S A *108*, 15647–15654. https://doi.org/10.1073/pnas.1014269108.

93. Watabe-Uchida, M., and Uchida, N. (2018). Multiple Dopamine Systems: Weal and Woe of Dopamine. Cold Spring Harb. Symp. Quant. Biol. *83*, 83–95. https://doi.org/10.1101/sqb.2018.83.037648.

94. Castell, L., Rogliardo, A., Borgne, T.L., Naon, C., Cathala, A., Puighermanal, E., Makrini, L., Mashhour, N., Petit, C.P., Bernat, C., et al. (2024). Midbrain dopamine D2R regulates the salience of threat-related events. Preprint, https://doi.org/10.1101/2024.11.12.623233 https://doi.org/10.1101/2024.11.12.623233.

95. Kong, E., Monje, F.J., Hirsch, J., and Pollak, D.D. (2014). Learning not to Fear: Neural Correlates of Learned Safety. Neuropsychopharmacol *39*, 515–527. https://doi.org/10.1038/npp.2013.191.

96. Li, S., and Kirouac, G.J. (2008). Projections from the paraventricular nucleus of the thalamus to the forebrain, with special emphasis on the extended amygdala. Journal of Comparative Neurology *506*, 263–287. https://doi.org/10.1002/cne.21502.

97. Vertes, R.P., Linley, S.B., and Hoover, W.B. (2015). LIMBIC CIRCUITRY OF THE MIDLINE THALAMUS. Neurosci Biobehav Rev *54*, 89–107. https://doi.org/10.1016/j.neubiorev.2015.01.014.

98. Van der Werf, Y.D., Witter, M.P., and Groenewegen, H.J. (2002). The intralaminar and midline nuclei of the thalamus. Anatomical and functional evidence for participation in processes of arousal and awareness. Brain Research Reviews *39*, 107–140. https://doi.org/10.1016/S0165-0173(02)00181-9.

99. Pinto, A., Jankowski, M., and Sesack, S.R. (2003). Projections from the paraventricular nucleus of the thalamus to the rat prefrontal cortex and nucleus accumbens shell: Ultrastructural characteristics and spatial relationships with dopamine afferents. Journal of Comparative Neurology *459*, 142–155. https://doi.org/10.1002/cne.10596.

100. Parsons, M.P., Li, S., and Kirouac, G.J. (2007). Functional and anatomical connection between the paraventricular nucleus of the thalamus and dopamine fibers of the nucleus accumbens. Journal of Comparative Neurology *500*, 1050–1063. https://doi.org/10.1002/cne.21224.

101. Clark, A.M., Leroy, F., Martyniuk, K.M., Feng, W., McManus, E., Bailey, M.R., Javitch, J.A., Balsam, P.D., and Kellendonk, C. (2017). Dopamine D2 Receptors in the Paraventricular Thalamus Attenuate Cocaine Locomotor Sensitization. eNeuro *4*, ENEURO.0227-17.2017. https://doi.org/10.1523/ENEURO.0227-17.2017.

102. Macdonald, E.E., Ma, J., Liu, D., Yu, K., Authement, M.E., Leng, Y., Goldbach, H.C., Alvarez, V.A., Averbeck, B.B., and Penzo, M.A. (2025). A synaptic mechanism for encoding the learned value of action-derived safety. bioRxiv, 2025.08.04.668532. https://doi.org/10.1101/2025.08.04.668532.

103. Kapur, S., Mizrahi, R., and Li, M. (2005). From dopamine to salience to psychosis—linking biology, pharmacology and phenomenology of psychosis. Schizophrenia Research *79*, 59–68. https://doi.org/10.1016/j.schres.2005.01.003.

104. Ostroff, L.E., Cain, C.K., Bedont, J., Monfils, M.H., and Ledoux, J.E. (2010). Fear and safety learning differentially affect synapse size and dendritic translation in the lateral amygdala. Proc Natl Acad Sci U S A *107*, 9418–9423. https://doi.org/10.1073/pnas.0913384107.

105. Pollak, D.D., Monje, F.J., Zuckerman, L., Denny, C.A., Drew, M.R., and Kandel, E.R. (2008). An animal model of a behavioral intervention for depression. Neuron *60*, 149–161. https://doi.org/10.1016/j.neuron.2008.07.041.

106. Oleson, E.B., Gentry, R.N., Chioma, V.C., and Cheer, J.F. (2012). Subsecond dopamine release in the nucleus accumbens predicts conditioned punishment and its successful avoidance. J Neurosci *32*, 14804–14808. https://doi.org/10.1523/JNEUROSCI.3087-12.2012.

107. Wenzel, J.M., Oleson, E.B., Gove, W.N., Cole, A.B., Gyawali, U., Dantrassy, H.M., Bluett, R.J., Dryanovski, D.I., Stuber, G.D., Deisseroth, K., et al. (2018). Phasic Dopamine Signals in the Nucleus Accumbens that Cause Active Avoidance Require Endocannabinoid Mobilization in the Midbrain. Curr Biol *28*, 1392-1404.e5. https://doi.org/10.1016/j.cub.2018.03.037.

108. De Bundel, D., Zussy, C., Espallergues, J., Gerfen, C.R., Girault, J.-A., and Valjent, E. (2016). Dopamine D2 receptors gate generalization of conditioned threat responses through mTORC1 signaling in the extended amygdala. Mol Psychiatry *21*, 1545–1553. https://doi.org/10.1038/mp.2015.210.

109. Phelps, E.A., and Sharot, T. (2008). How (and Why) Emotion Enhances the Subjective Sense of Recollection. Curr Dir Psychol Sci *17*, 147–152. https://doi.org/10.1111/j.1467-8721.2008.00565.x.

110. Santangelo, V. (2015). Forced to remember: When memory is biased by salient information. Behavioural Brain Research *283*, 1–10. https://doi.org/10.1016/j.bbr.2015.01.013.

1025 111. Ghazizadeh, A., and Hikosaka, O. (2022). Salience memories formed by value, novelty and
1026 aversiveness jointly shape object responses in the prefrontal cortex and basal ganglia. Nat
1027 Commun *13*, 6338. https://doi.org/10.1038/s41467-022-33514-3.

1028 112. Sharot, T., Riccardi, A.M., Raio, C.M., and Phelps, E.A. (2007). Neural mechanisms
1029 mediating optimism bias. Nature *450*, 102–105. https://doi.org/10.1038/nature06280.

1030 113. Dunsmoor, J.E., Murty, V.P., Clewett, D., Phelps, E.A., and Davachi, L. (2022). Tag and
1031 Capture: How salient experiences target and rescue nearby events in memory. Trends Cogn Sci
1032 *26*, 782–795. https://doi.org/10.1016/j.tics.2022.06.009.

1033 114. Colavito, V., Tesoriero, C., Wirtu, A.T., Grassi-Zucconi, G., and Bentivoglio, M. (2015). Limbic
1034 thalamus and state-dependent behavior: The paraventricular nucleus of the thalamic midline as a
1035 node in circadian timing and sleep/wake-regulatory networks. Neuroscience & Biobehavioral
1036 Reviews *54*, 3–17. https://doi.org/10.1016/j.neubiorev.2014.11.021.

1037 115. Ren, S., Wang, Y., Yue, F., Cheng, X., Dang, R., Qiao, Q., Sun, X., Li, X., Jiang, Q., Yao, J.,
1038 et al. (2018). The paraventricular thalamus is a critical thalamic area for wakefulness. Science *362*,
1039 429–434. https://doi.org/10.1126/science.aat2512.

1040 116. Paniccia, J.E., Vollmer, K.M., Green, L.M., Grant, R.I., Winston, K.T., Buchmaier, S.,
1041 Westphal, A.M., Clarke, R.E., Doncheck, E.M., Bordieanu, B., et al. (2024). Restoration of a
1042 paraventricular thalamo-accumbal behavioral suppression circuit prevents reinstatement of heroin
1043 seeking. Neuron *112*, 772-785.e9. https://doi.org/10.1016/j.neuron.2023.11.024.

1044 117. Vollmer, K.M., Green, L.M., Grant, R.I., Winston, K.T., Doncheck, E.M., Bowen, C.W.,
1045 Paniccia, J.E., Clarke, R.E., Tiller, A., Siegler, P.N., et al. (2022). An opioid-gated
1046 thalamoaccumbal circuit for the suppression of reward seeking in mice. Nat Commun *13*, 6865.
1047 https://doi.org/10.1038/s41467-022-34517-w.

1048 118. McGinty, J.F., and Otis, J.M. (2020). Heterogeneity in the Paraventricular Thalamus: The
1049 Traffic Light of Motivated Behaviors. Front. Behav. Neurosci. *14*.
1050 https://doi.org/10.3389/fnbeh.2020.590528.

1051 119. Otis, J.M., Namboodiri, V.M.K., Matan, A.M., Voets, E.S., Mohorn, E.P., Kosyk, O., McHenry,
1052 J.A., Robinson, J.E., Resendez, S.L., Rossi, M.A., et al. (2017). Prefrontal cortex output circuits
1053 guide reward seeking through divergent cue encoding. Nature *543*, 103–107.
1054 https://doi.org/10.1038/nature21376.

1055 120. Beas, S., Khan, I., Gao, C., Loewinger, G., Macdonald, E., Bashford, A., Rodriguez-
1056 Gonzalez, S., Pereira, F., and Penzo, M.A. (2024). Dissociable encoding of motivated behavior by
1057 parallel thalamo-striatal projections. Current Biology *34*, 1549-1560.e3.
1058 https://doi.org/10.1016/j.cub.2024.02.037.

1059 121. Brewin, C.R. (2001). A cognitive neuroscience account of posttraumatic stress disorder and
1060 its treatment. Behaviour Research and Therapy *39*, 373–393. https://doi.org/10.1016/S0005-
1061 7967(00)00087-5.

1062 122. Layton, B., and Krikorian, R. (2002). Memory mechanisms in posttraumatic stress disorder. J
1063 Neuropsychiatry Clin Neurosci *14*, 254–261. https://doi.org/10.1176/jnp.14.3.254.

1064 123. Puighermanal Emma, Biever Anne, Espallergues Julie, Gangarossa Giuseppe, De Bundel
1065 Dimitri, and Valjent Emmanuel (2014). drd2-cre:ribotag mouse line unravels the possible diversity
1066 of dopamine d2 receptor-expressing cells of the dorsal mouse hippocampus. Hippocampus *25*,
1067 858–875. https://doi.org/10.1002/hipo.22408.

1068 124. Trouche, S., Sasaki, J.M., Tu, T., and Reijmers, L.G. (2013). Fear extinction causes target-
1069 specific remodeling of perisomatic inhibitory synapses. Neuron *80*.
1070 https://doi.org/10.1016/j.neuron.2013.07.047.

1071 125. Han, S., Soleiman, M.T., Soden, M.E., Zweifel, L.S., and Palmiter, R.D. (2015). Elucidating an
1072 Affective Pain Circuit That Creates a Threat Memory. Cell *162*, 363–374.
1073 https://doi.org/10.1016/j.cell.2015.05.057.

1074

Figure 1

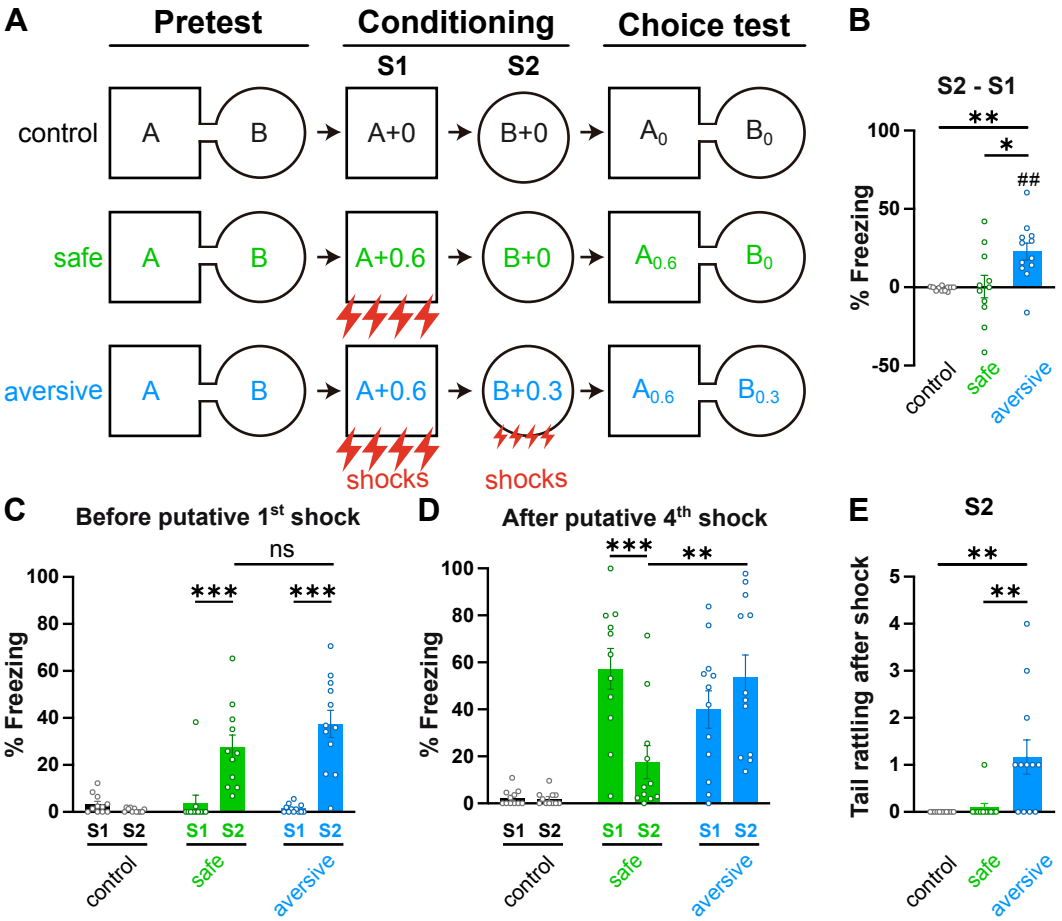
A
Pretest
Conditioning
Choice test
S1
S2
control
safe
aversive
A
B
A+0
B+0
A0
B0
A+0.6
A0.6
B0
B+0.3
B0.3
shocks
shocks
B
S2 - S1
% Freezing
control
safe
aversive
C
Before putative 1st shock
ns
% Freezing
S1 S2
control
safe
aversive
D
After putative 4th shock
% Freezing
E
S2
Tail rattling after shock

Figure S1

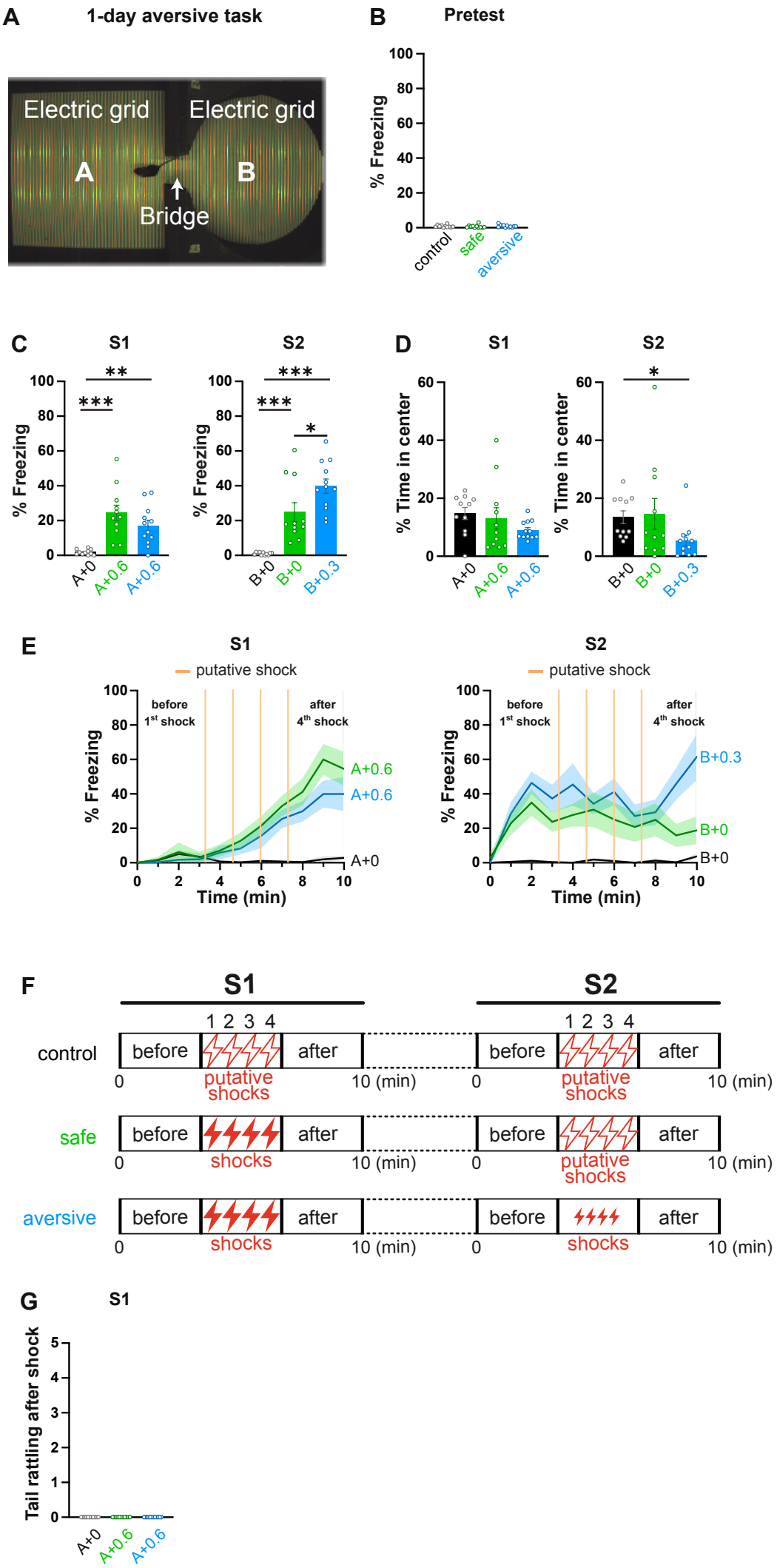
A
1-day aversive task
Electric grid
Electric grid
A
B
Bridge
B
Pretest
% Freezing
control
safe
aversive
C
S1
S2
% Freezing
A+0
A+0.6
A+0.6
B+0
B+0
B+0.3
D
S1
S2
% Time in center
E
S1
S2
putative shock
before 1st shock
after 4th shock
% Freezing
Time (min)
A+0.6
A+0.6
A+0
B+0.3
B+0
B+0
F
S1
S2
control
safe
aversive
before
after
putative shocks
shocks
10 (min)
G
S1
Tail rattling after shock

Figure 2

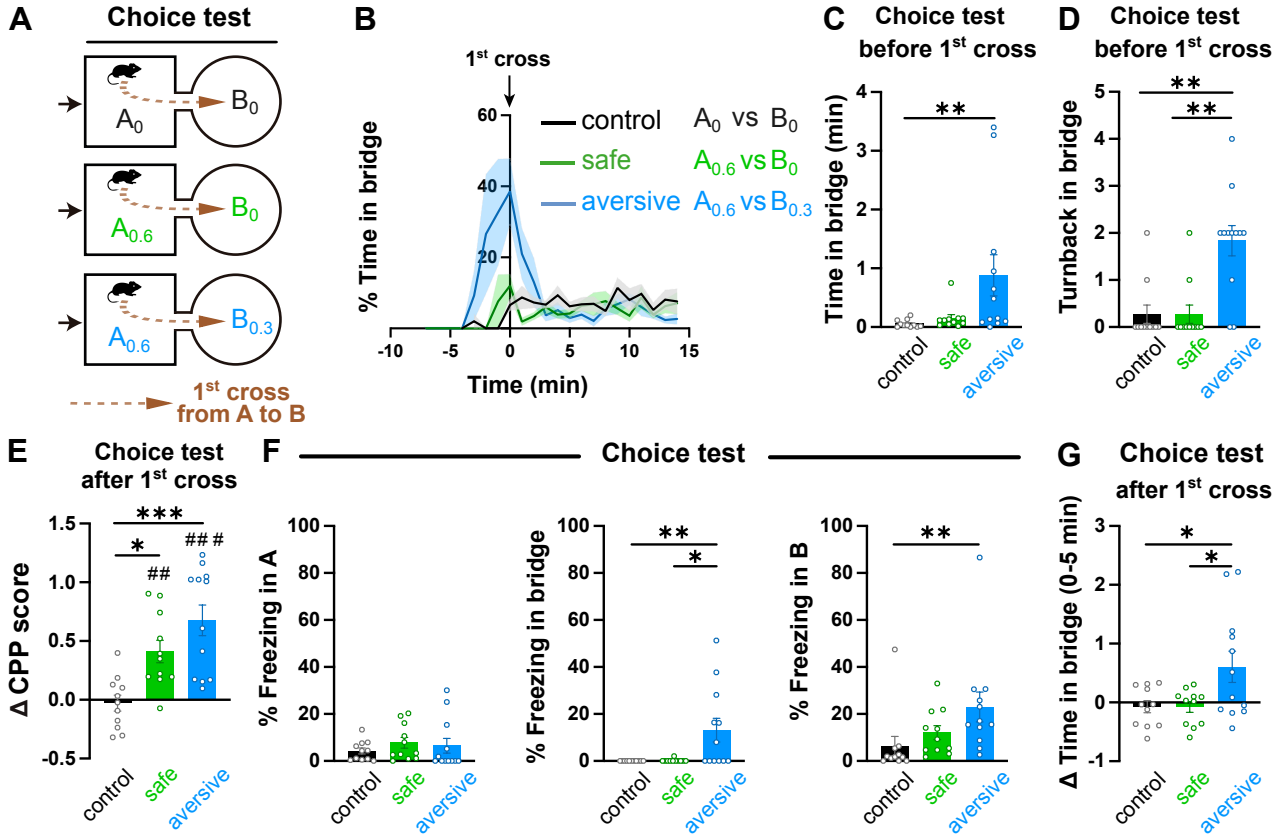
A
Choice test
A0
B0
A0.6
B0
A0.6
B0.3
1st cross from A to B
B
1st cross
% Time in bridge
Time (min)
control
safe
aversive
A0 vs B0
A0.6 vs B0
A0.6 vs B0.3
C
Choice test before 1st cross
Time in bridge (min)
D
Choice test before 1st cross
Turnback in bridge
E
Choice test after 1st cross
Δ CPP score
F
Choice test
% Freezing in A
% Freezing in bridge
% Freezing in B
G
Choice test after 1st cross
Δ Time in bridge (0-5 min)

Figure S2

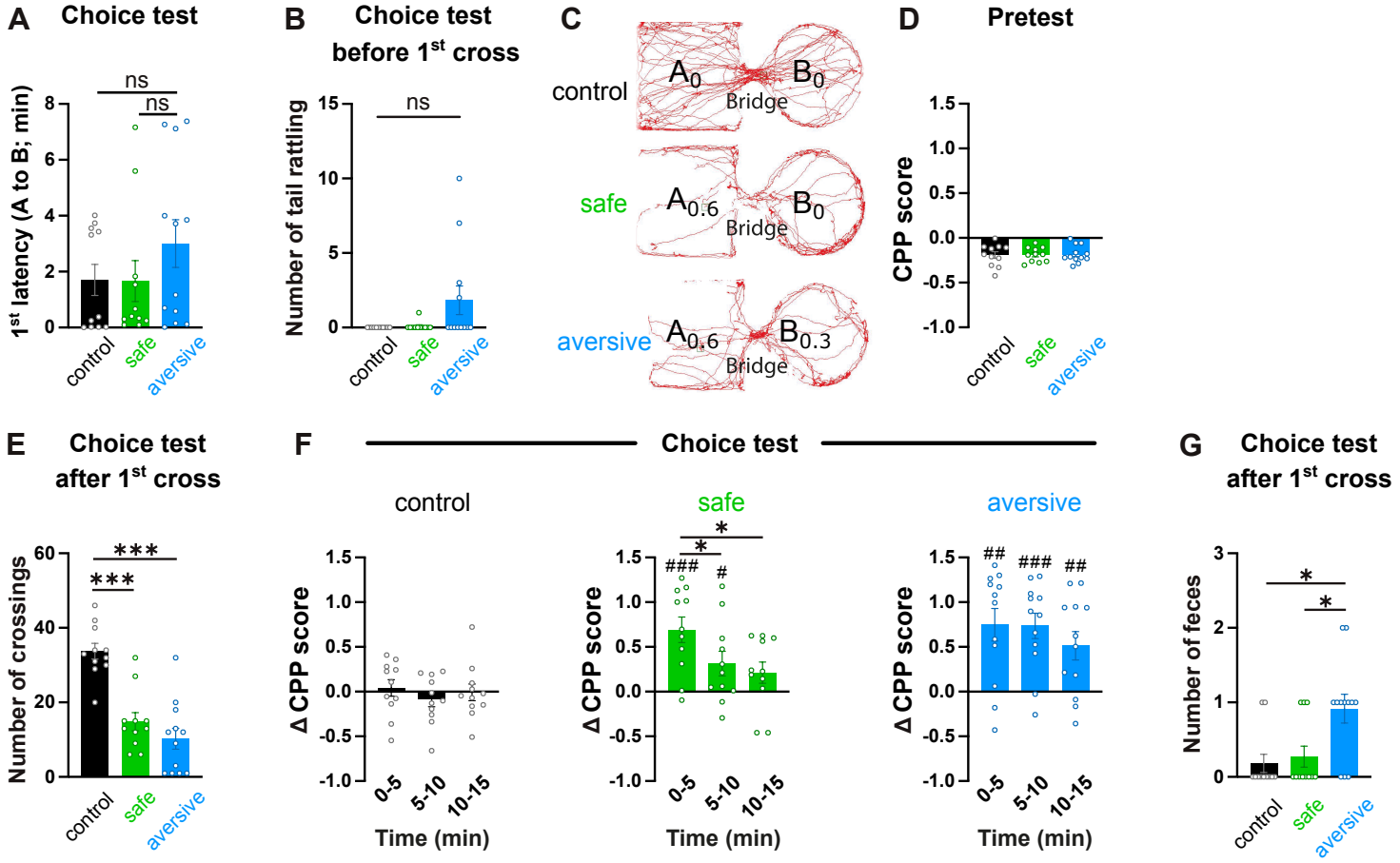
A
Choice test
1st latency (A to B; min)
ns
ns
control
safe
aversive
B
Choice test before 1st cross
Number of tail rattling
ns
control
safe
aversive
C
control
safe
aversive
A0
B0
A0.6
B0
A0.6
B0.3
Bridge
D
Pretest
CPP score
control
safe
aversive
E
Choice test after 1st cross
Number of crossings
***
***
control
safe
aversive
F
Choice test
control
safe
aversive
Δ CPP score
Time (min)
0-5
5-10
10-15
*
*
###
#
##
###
##
G
Choice test after 1st cross
Number of feces
*
*
control
safe
aversive

Figure 3

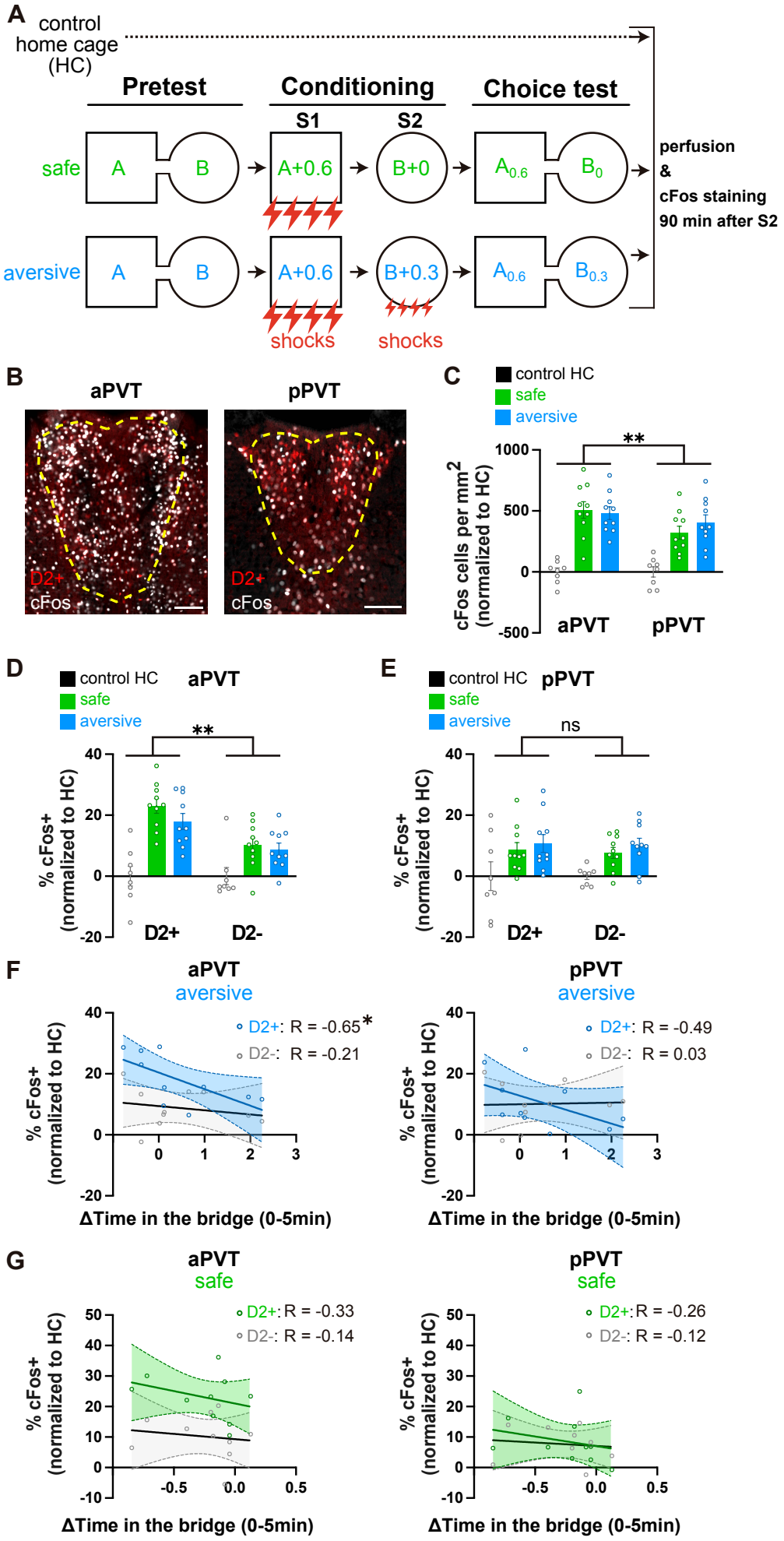
A
control
home cage
(HC)
Pretest
Conditioning
Choice test
S1
S2
safe
A
B
A+0.6
B+0
A0.6
B0
aversive
A
B
A+0.6
B+0.3
A0.6
B0.3
shocks
shocks
perfusion
&
cFos staining
90 min after S2
B
aPVT
pPVT
D2+
cFos
D2+
cFos
C
control HC
safe
aversive
**
cFos cells per mm2
(normalized to HC)
1000
500
0
-500
aPVT
pPVT
D
control HC
safe
aversive
aPVT
**
% cFos+
(normalized to HC)
40
20
0
-20
D2+
D2-
E
control HC
safe
aversive
pPVT
ns
% cFos+
(normalized to HC)
40
20
0
-20
D2+
D2-
F
aPVT
aversive
D2+: R = -0.65*
D2-: R = -0.21
% cFos+
(normalized to HC)
ΔTime in the bridge (0-5min)
pPVT
aversive
D2+: R = -0.49
D2-: R = 0.03
% cFos+
(normalized to HC)
ΔTime in the bridge (0-5min)
G
aPVT
safe
D2+: R = -0.33
D2-: R = -0.14
% cFos+
(normalized to HC)
ΔTime in the bridge (0-5min)
pPVT
safe
D2+: R = -0.26
D2-: R = -0.12
% cFos+
(normalized to HC)
ΔTime in the bridge (0-5min)

Figure S3

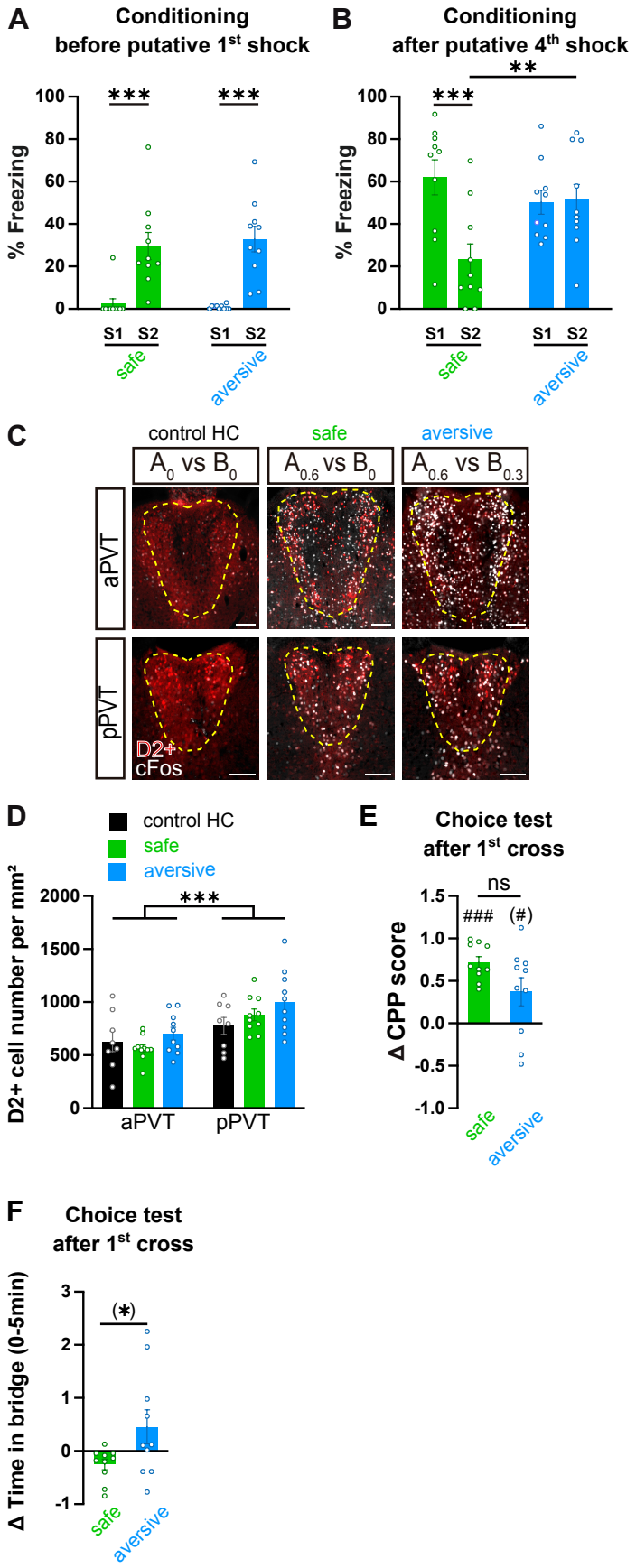
A
Conditioning
before putative 1st shock
% Freezing
100
80
60
40
20
0
***
***
S1 S2
S1 S2
safe
aversive
B
Conditioning
after putative 4th shock
**
***
% Freezing
S1 S2
S1 S2
safe
aversive
C
control HC
safe
aversive
A0 vs B0
A0.6 vs B0
A0.6 vs B0.3
aPVT
pPVT
D2+
cFos
D
control HC
safe
aversive
D2+ cell number per mm²
2000
1500
1000
500
0
***
aPVT
pPVT
E
Choice test
after 1st cross
ns
###
(#)
Δ CPP score
1.5
1.0
0.5
0.0
-0.5
-1.0
safe
aversive
F
Choice test
after 1st cross
Δ Time in bridge (0-5min)
3
2
1
0
-1
(*)
safe
aversive

Figure 4

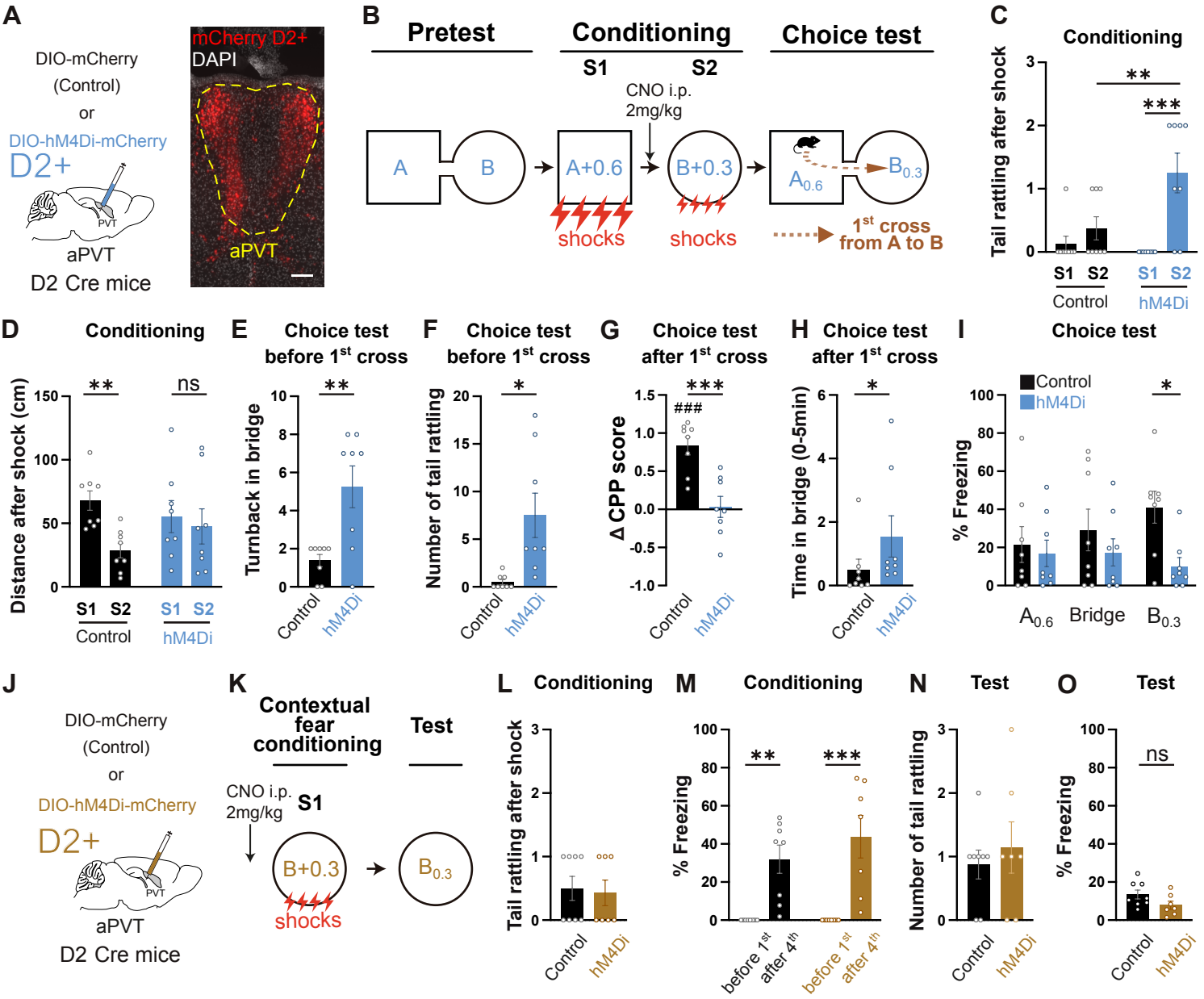
A
DIO-mCherry
(Control)
or
DIO-hM4Di-mCherry
D2+
PVT
aPVT
D2 Cre mice
mCherry D2+
DAPI
aPVT
B
Pretest
Conditioning
Choice test
S1
S2
CNO i.p.
2mg/kg
A
B
A+0.6
B+0.3
shocks
shocks
A0.6
B0.3
1st cross
from A to B
C
Conditioning
Tail rattling after shock
**
***
S1 S2
Control
S1 S2
hM4Di
D
Conditioning
Distance after shock (cm)
**
ns
S1 S2
Control
S1 S2
hM4Di
E
Choice test
before 1st cross
Turnback in bridge
**
Control
hM4Di
F
Choice test
before 1st cross
Number of tail rattling
*
Control
hM4Di
G
Choice test
after 1st cross
Δ CPP score
***
###
Control
hM4Di
H
Choice test
after 1st cross
Time in bridge (0-5min)
*
Control
hM4Di
I
Choice test
Control
hM4Di
% Freezing
*
A0.6
Bridge
B0.3
J
DIO-mCherry
(Control)
or
DIO-hM4Di-mCherry
D2+
PVT
aPVT
D2 Cre mice
K
Contextual
fear
conditioning
Test
CNO i.p.
2mg/kg
S1
B+0.3
shocks
B0.3
L
Conditioning
Tail rattling after shock
Control
hM4Di
M
Conditioning
% Freezing
**
***
before 1st
after 4th
before 1st
after 4th
N
Test
Number of tail rattling
Control
hM4Di
O
Test
% Freezing
ns
Control
hM4Di

Figure S4

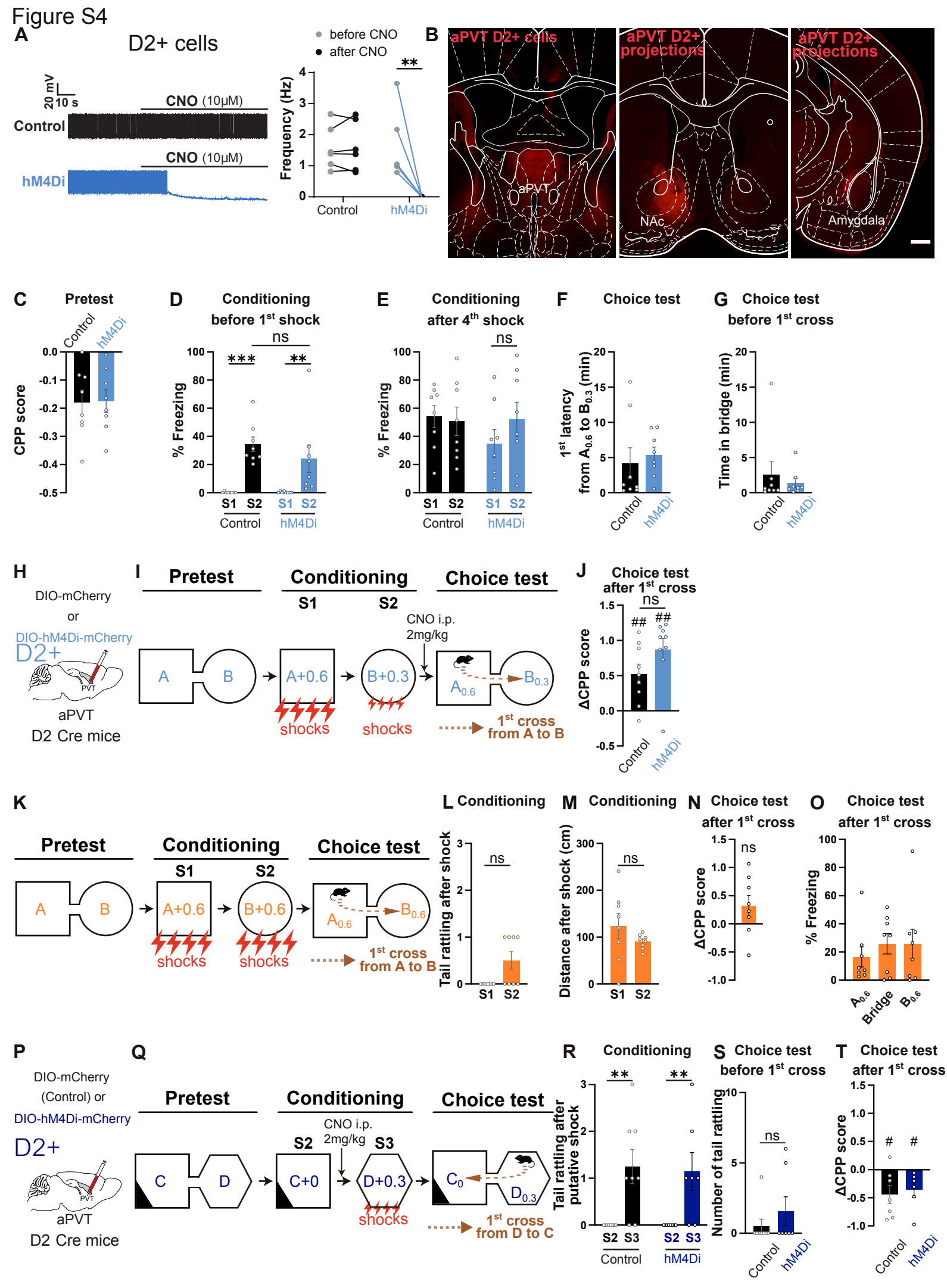
A
D2+ cells
20 mV
10 s
CNO (10μM)
Control
CNO (10μM)
hM4Di
before CNO
after CNO
Frequency (Hz)
Control
hM4Di
B
aPVT D2+ cells
aPVT
aPVT D2+ projections
NAc
aPVT D2+ projections
Amygdala
C
Pretest
CPP score
Control
hM4Di
D
Conditioning before 1st shock
% Freezing
ns
S1 S2
Control
hM4Di
E
Conditioning after 4th shock
% Freezing
F
Choice test
1st latency from A0.6 to B0.3 (min)
G
Choice test before 1st cross
Time in bridge (min)
H
DIO-mCherry
or
DIO-hM4Di-mCherry
D2+
PVT
aPVT
D2 Cre mice
I
Pretest
Conditioning
Choice test
S1
S2
CNO i.p.
2mg/kg
A
B
A+0.6
B+0.3
A0.6
B0.3
shocks
shocks
1st cross from A to B
J
Choice test after 1st cross
ΔCPP score
K
Pretest
Conditioning
Choice test
S1
S2
A
B
A+0.6
B+0.6
A0.6
B0.6
shocks
shocks
1st cross from A to B
L
Conditioning
Tail rattling after shock
M
Conditioning
Distance after shock (cm)
N
Choice test after 1st cross
ΔCPP score
O
Choice test after 1st cross
% Freezing
A0.6
Bridge
B0.6
P
DIO-mCherry
(Control) or
DIO-hM4Di-mCherry
D2+
PVT
aPVT
D2 Cre mice
Q
Pretest
Conditioning
Choice test
CNO i.p.
2mg/kg
S2
S3
C
D
C+0
D+0.3
C0
D0.3
shocks
1st cross from D to C
R
Conditioning
Tail rattling after putative shock
S2 S3
Control
hM4Di
S
Choice test before 1st cross
Number of tail rattling
T
Choice test after 1st cross
ΔCPP score

Figure 5

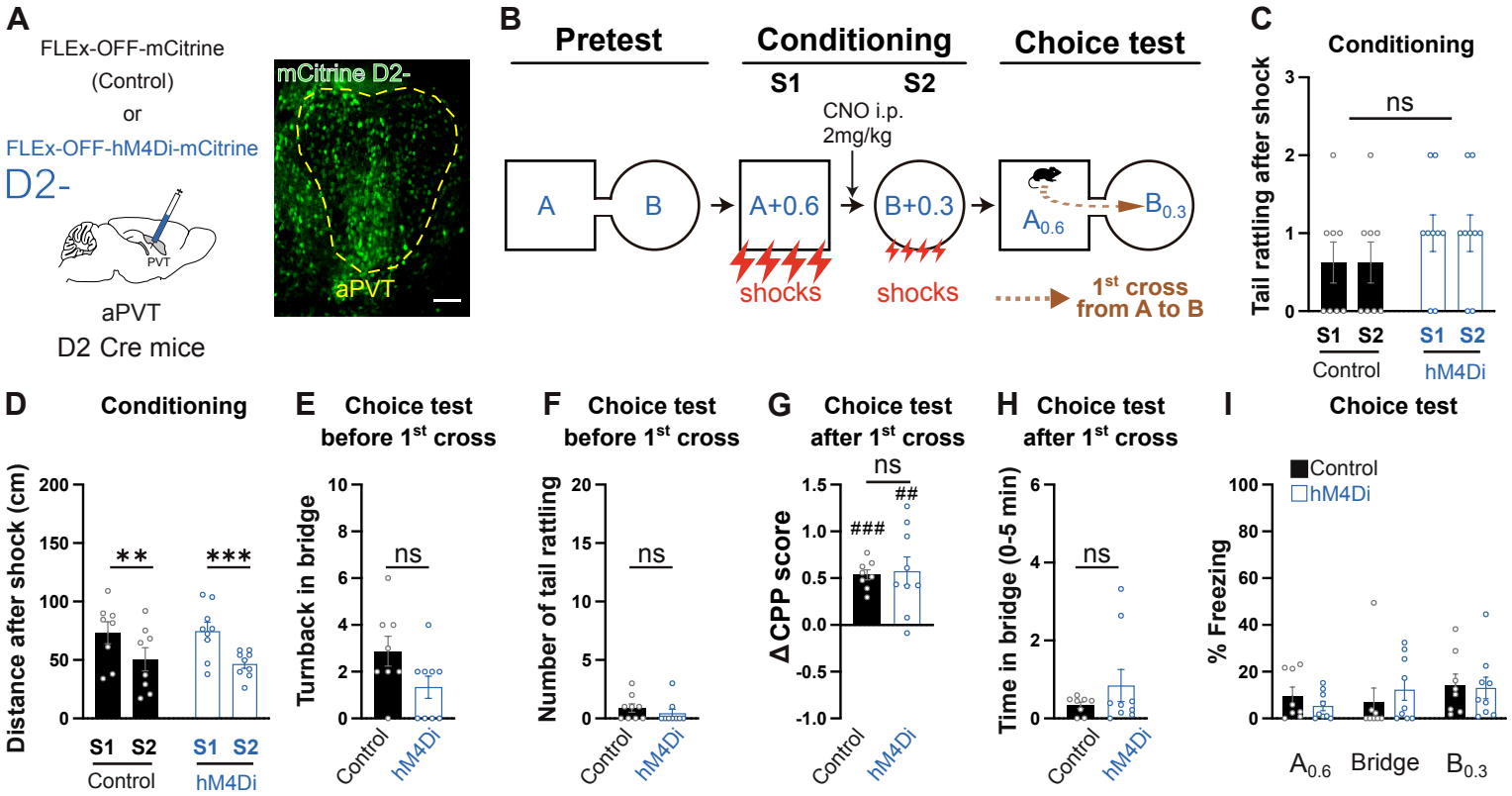
A
FLEx-OFF-mCitrine
(Control)
or
FLEx-OFF-hM4Di-mCitrine
D2-
PVT
aPVT
D2 Cre mice
mCitrine D2-
aPVT
B
Pretest
Conditioning
Choice test
S1
S2
CNO i.p.
2mg/kg
A
B
A+0.6
B+0.3
shocks
shocks
A0.6
B0.3
1st cross
from A to B
C
Conditioning
Tail rattling after shock
ns
S1 S2
Control
S1 S2
hM4Di
D
Conditioning
Distance after shock (cm)
**
***
S1 S2
Control
S1 S2
hM4Di
E
Choice test
before 1st cross
Turnback in bridge
ns
Control
hM4Di
F
Choice test
before 1st cross
Number of tail rattling
ns
Control
hM4Di
G
Choice test
after 1st cross
ΔCPP score
ns
###
##
Control
hM4Di
H
Choice test
after 1st cross
Time in bridge (0-5 min)
ns
Control
hM4Di
I
Choice test
Control
hM4Di
% Freezing
A0.6
Bridge
B0.3

Figure S5

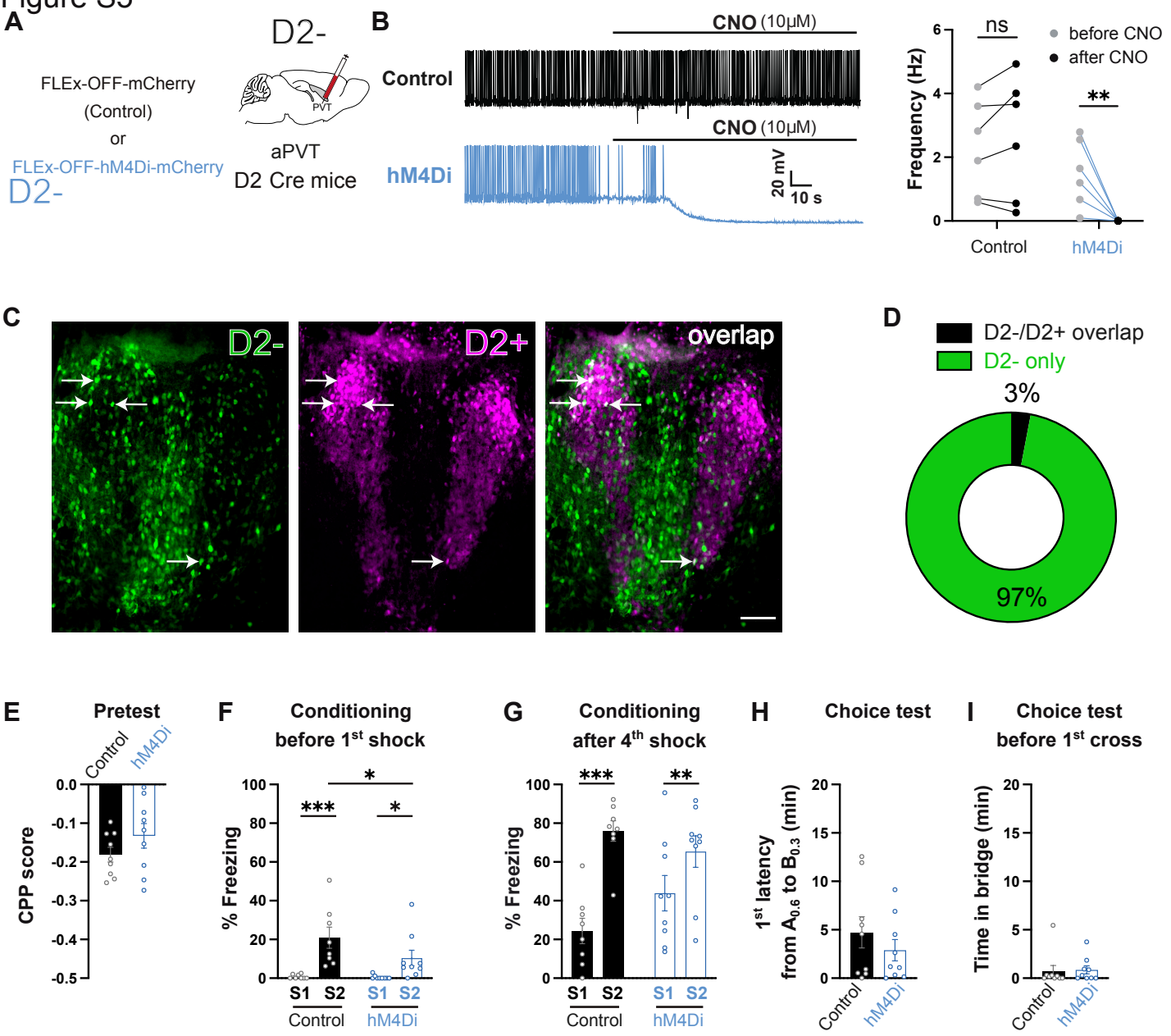
A
D2-
FLEx-OFF-mCherry
(Control)
or
FLEx-OFF-hM4Di-mCherry
D2-
PVT
aPVT
D2 Cre mice
B
CNO (10μM)
Control
CNO (10μM)
hM4Di
20 mV
10 s
ns
before CNO
after CNO
**
Frequency (Hz)
Control
hM4Di
C
D2-
D2+
overlap
D
D2-/D2+ overlap
D2- only
3%
97%
E
Pretest
Control
hM4Di
CPP score
F
Conditioning
before 1st shock
% Freezing
S1 S2 S1 S2
Control
hM4Di
G
Conditioning
after 4th shock
% Freezing
S1 S2 S1 S2
Control
hM4Di
H
Choice test
1st latency
from A0.6 to B0.3 (min)
Control
hM4Di
I
Choice test
before 1st cross
Time in bridge (min)
Control
hM4Di

Figure 6

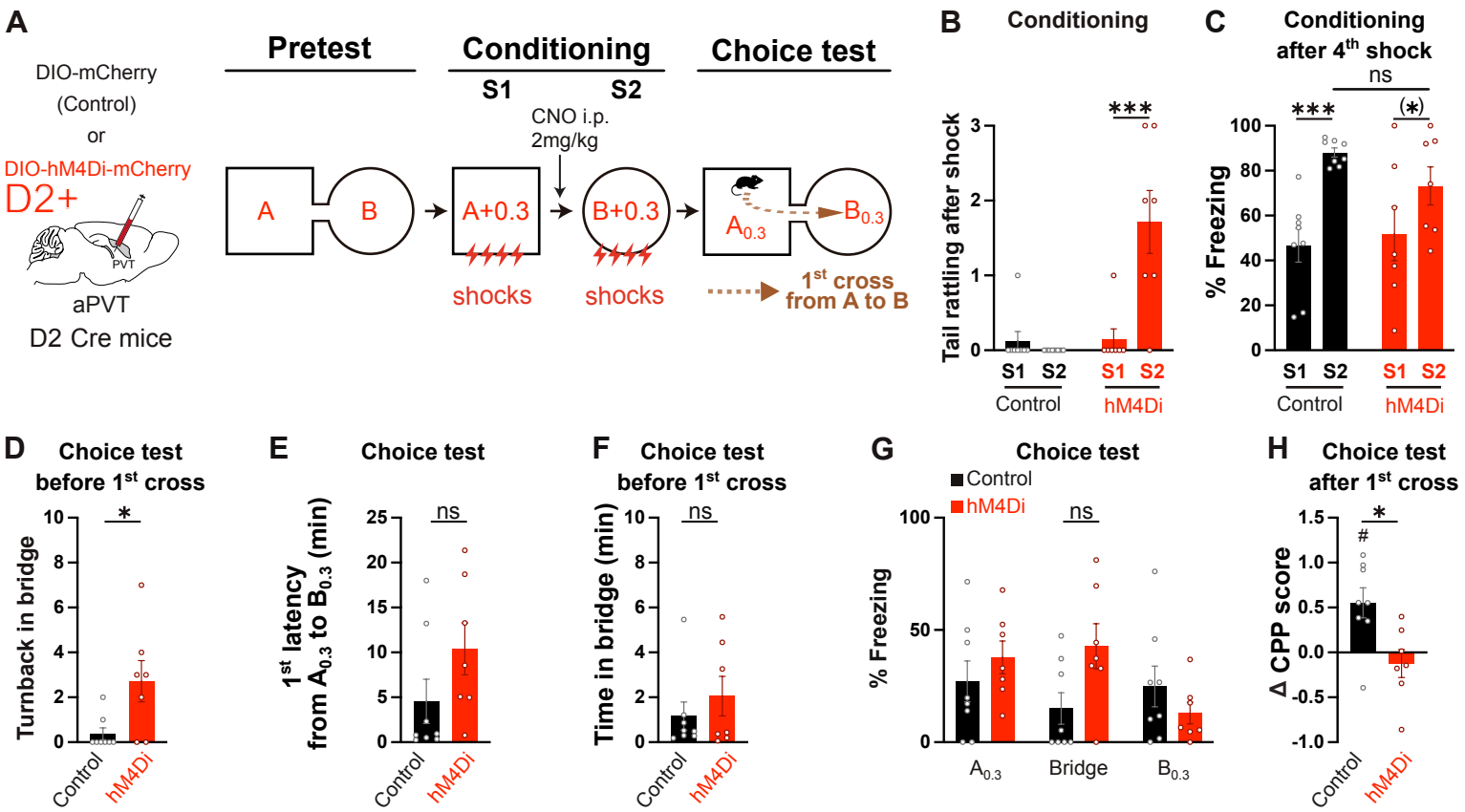
A
DIO-mCherry
(Control)
or
DIO-hM4Di-mCherry
D2+
PVT
aPVT
D2 Cre mice
Pretest
Conditioning
S1
S2
CNO i.p.
2mg/kg
Choice test
A
B
A+0.3
B+0.3
shocks
shocks
A0.3
B0.3
1st cross
from A to B
B
Conditioning
Tail rattling after shock
***
S1 S2 S1 S2
Control
hM4Di
C
Conditioning
after 4th shock
ns
***
(*)
% Freezing
S1 S2 S1 S2
Control
hM4Di
D
Choice test
before 1st cross
Turnback in bridge
*
Control
hM4Di
E
Choice test
1st latency
from A0.3 to B0.3 (min)
ns
Control
hM4Di
F
Choice test
before 1st cross
Time in bridge (min)
ns
Control
hM4Di
G
Choice test
Control
hM4Di
% Freezing
ns
A0.3
Bridge
B0.3
H
Choice test
after 1st cross
Δ CPP score
*
#
Control
hM4Di

Figure S6

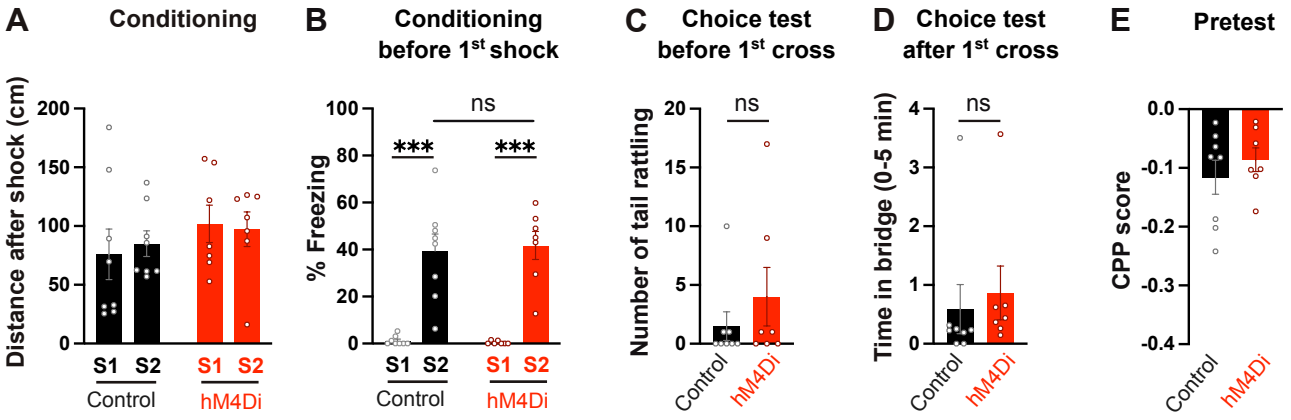
A
Conditioning
Distance after shock (cm)
200
150
100
50
0
S1 S2
Control
S1 S2
hM4Di
B
Conditioning before 1st shock
% Freezing
100
80
60
40
20
0
ns
***
***
S1 S2
Control
S1 S2
hM4Di
C
Choice test before 1st cross
Number of tail rattling
20
15
10
5
0
ns
Control
hM4Di
D
Choice test after 1st cross
Time in bridge (0-5 min)
4
3
2
1
0
ns
Control
hM4Di
E
Pretest
CPP score
0.0
-0.1
-0.2
-0.3
-0.4
Control
hM4Di

Figure 7

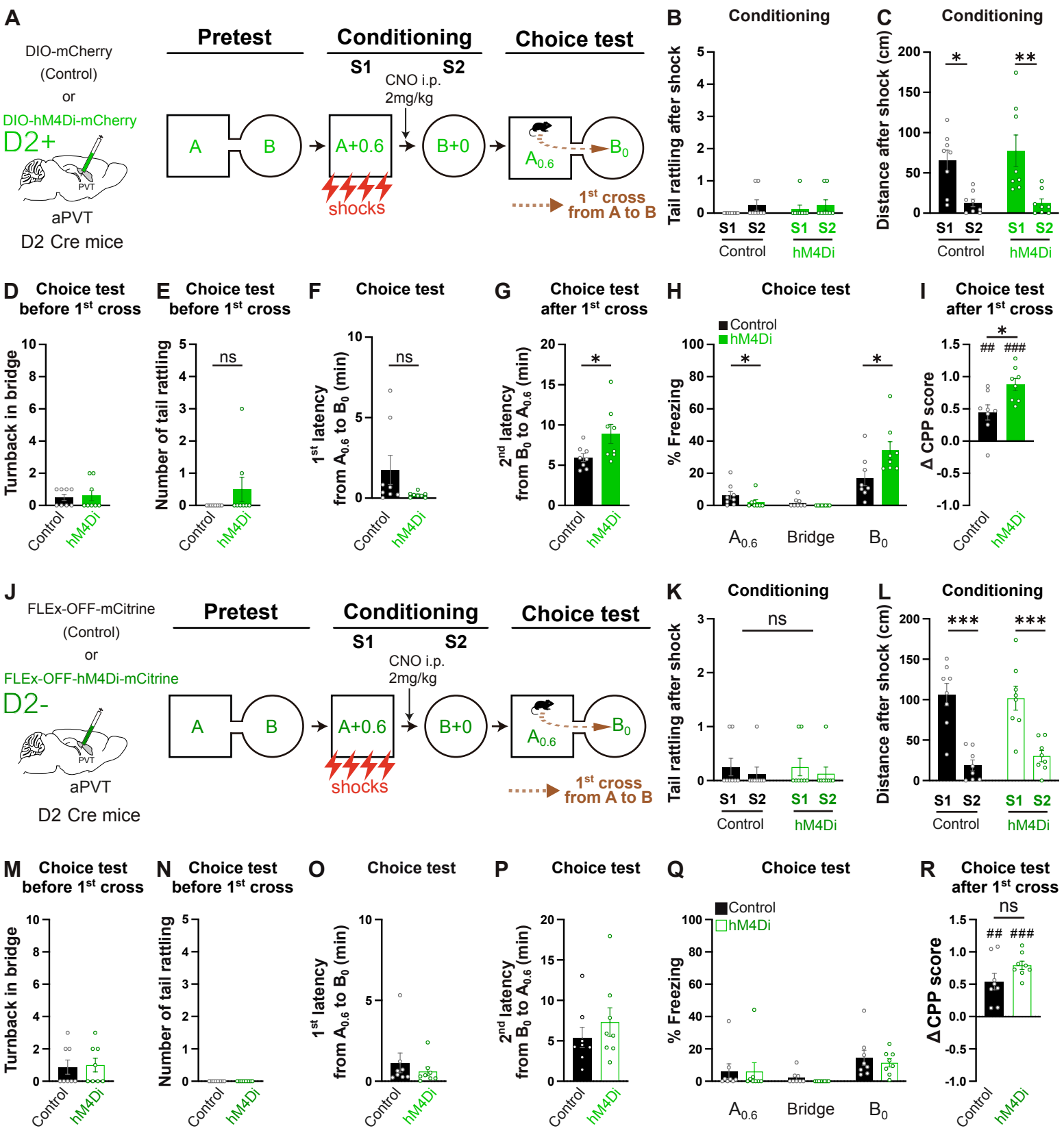
A
DIO-mCherry
(Control)
or
DIO-hM4Di-mCherry
D2+
PVT
aPVT
D2 Cre mice
Pretest
Conditioning
Choice test
S1
S2
CNO i.p.
2mg/kg
A
B
A+0.6
B+0
A0.6
B0
shocks
1st cross
from A to B
B
Conditioning
Tail rattling after shock
S1 S2 S1 S2
Control hM4Di
C
Conditioning
Distance after shock (cm)
*
**
S1 S2 S1 S2
Control hM4Di
D
Choice test
before 1st cross
Turnback in bridge
Control
hM4Di
E
Choice test
before 1st cross
Number of tail rattling
ns
F
Choice test
1st latency
from A0.6 to B0 (min)
ns
G
Choice test
after 1st cross
2nd latency
from B0 to A0.6 (min)
*
H
Choice test
Control
hM4Di
% Freezing
*
*
A0.6
Bridge
B0
I
Choice test
after 1st cross
Δ CPP score
*
##
###
J
FLEx-OFF-mCitrine
(Control)
or
FLEx-OFF-hM4Di-mCitrine
D2-
PVT
aPVT
D2 Cre mice
Pretest
Conditioning
Choice test
S1
S2
CNO i.p.
2mg/kg
A
B
A+0.6
B+0
A0.6
B0
shocks
1st cross
from A to B
K
Conditioning
Tail rattling after shock
ns
S1 S2 S1 S2
Control hM4Di
L
Conditioning
Distance after shock (cm)
***
***
S1 S2 S1 S2
Control hM4Di
M
Choice test
before 1st cross
Turnback in bridge
Control
hM4Di
N
Choice test
before 1st cross
Number of tail rattling
O
Choice test
1st latency
from A0.6 to B0 (min)
P
Choice test
2nd latency
from B0 to A0.6 (min)
Q
Choice test
Control
hM4Di
% Freezing
A0.6
Bridge
B0
R
Choice test
after 1st cross
ns
Δ CPP score
##
###

Figure S7

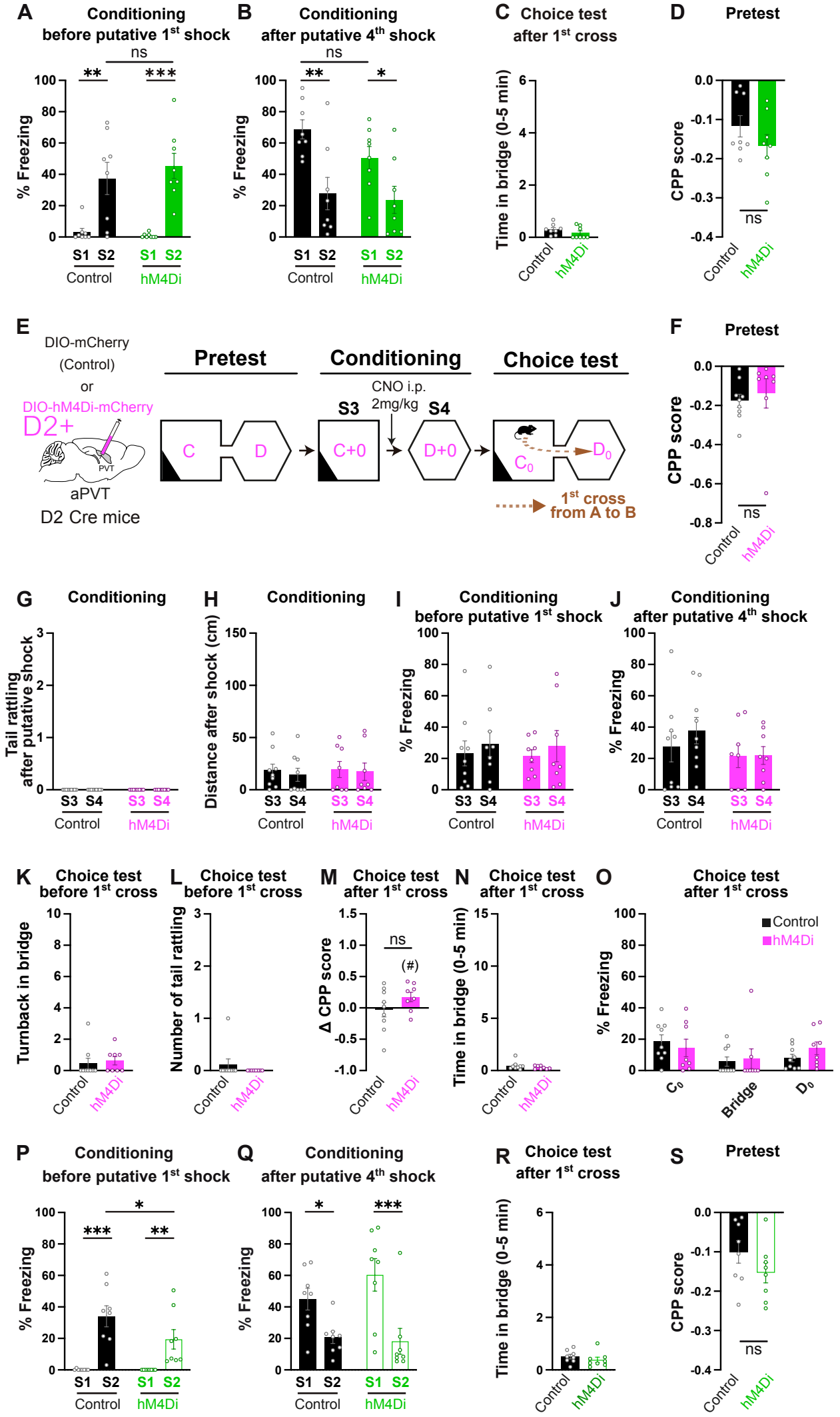
A
Conditioning
before putative 1st shock
ns
**
***
% Freezing
S1 S2
Control
S1 S2
hM4Di
B
Conditioning
after putative 4th shock
ns
**
*
% Freezing
S1 S2
Control
S1 S2
hM4Di
C
Choice test
after 1st cross
Time in bridge (0-5 min)
Control
hM4Di
D
Pretest
CPP score
ns
Control
hM4Di
E
DIO-mCherry
(Control)
or
DIO-hM4Di-mCherry
D2+
PVT
aPVT
D2 Cre mice
Pretest
Conditioning
Choice test
CNO i.p.
2mg/kg
S3
S4
C
D
C+0
D+0
C0
D0
1st cross
from A to B
F
Pretest
CPP score
ns
Control
hM4Di
G
Conditioning
Tail rattling
after putative shock
S3 S4
Control
S3 S4
hM4Di
H
Conditioning
Distance after shock (cm)
S3 S4
Control
S3 S4
hM4Di
I
Conditioning
before putative 1st shock
% Freezing
S3 S4
Control
S3 S4
hM4Di
J
Conditioning
after putative 4th shock
% Freezing
S3 S4
Control
S3 S4
hM4Di
K
Choice test
before 1st cross
Turnback in bridge
Control
hM4Di
L
Choice test
before 1st cross
Number of tail rattling
Control
hM4Di
M
Choice test
after 1st cross
Δ CPP score
ns
(#)
Control
hM4Di
N
Choice test
after 1st cross
Time in bridge (0-5 min)
Control
hM4Di
O
Choice test
after 1st cross
Control
hM4Di
% Freezing
C0
Bridge
D0
P
Conditioning
before putative 1st shock
*
***
**
% Freezing
S1 S2
Control
S1 S2
hM4Di
Q
Conditioning
after putative 4th shock
*
***
% Freezing
S1 S2
Control
S1 S2
hM4Di
R
Choice test
after 1st cross
Time in bridge (0-5 min)
Control
hM4Di
S
Pretest
CPP score
ns
Control
hM4Di